NUREG/CR-0412
TREE-1294
for U.S. Nuclear Regulatory Commission

TERA

# QUARTERLY TECHNICAL PROGRESS REPORT ON WATER REACTOR SAFETY PROGRAMS SPONSORED BY THE NUCLEAR REGULATORY COMMISSION'S DIVISION OF REACTOR SAFETY RESEARCH JULY—SEPTEMBER 1978

October 1978

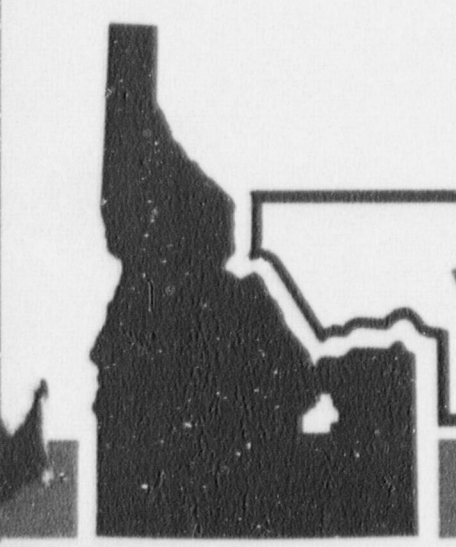

EG&G Idaho, Inc.

IDAHO NATIONAL ENGINEERING LABORATORY

DEPARTMENT OF ENERGY

IDAHO OPERATIONS OFFICE UNDER CONTRACT EY-76-C-07-1570

Available from
National Technical Information Service
Springfield, Virginia 22161
Price: Printed Copy A05; Microfiche $3.00

The price of this document for requesters outside the North American continent can be obtained from the National Technical Information Service.

NUREG/CR-0412
TREE-1294
R2, R3, and R4

# QUARTERLY TECHNICAL PROGRESS REPORT ON WATER REACTOR SAFETY PROGRAMS SPONSORED BY THE NUCLEAR REGULATORY COMMISSION'S DIVISION OF REACTOR SAFETY RESEARCH, JULY-SEPTEMBER 1978

L. J. Ybarrondo, Director
Water Reactor Research

Technical Editor - E. L. Wills

October 1978

Idaho National Engineering Laboratory
Idaho Falls, ID 83401
operated by
EG&G Idaho, Inc.
for the
U. S. Department of Energy
Idaho Operations Office

Prepared for the
U. S. Nuclear Regulatory Commission
Under Contract No. EY-76-C-07-1570

## ABSTRACT

Water reactor research performed by EG&G Idaho, Inc., July through September 1978 is summarized for ongoing programs: Semiscale, LOFT, Thermal Fuels Behavior, Code Development and Analysis, Code Assessment and Applications, and the 3-D Project. The Semiscale Program reports performance of four tests in the Mod-3 system and the application of a scanning densitometer for indicating two-phase flow regimes. The LOFT Experimental Program reports results from (a) the first series of LOFT nonnuclear experiments, (b) a predictive analysis for the first three LOFT nuclear tests, and (c) testing of flow measurement instrumentation. The Thermal Fuels Behavior Program reports completion of 20 reactivity-initiated accident tests and 4 related scoping tests in the Power Burst Facility reactor. The Code Development and Analysis Program reports development of the blowdown version of RELAP4/MOD7, application of the primary systems code RELAP5, and development of an analysis procedure for fuel rod input uncertainties for the FRAP-T5 code. The Code Assessment and Applications Program reports an assessment of the thermal-hydraulic code RELAP4/MOD6, completion of the fuel rod analysis code FRAPT-4 assessment, completion of a jet pump testing program, and expansion of the NRC/RSR data bank. The multinational 3-D Experiment Project reports development of specialized instrumentation in support of German and Japanese reflood experiments and completion of small-scale air-water tests to investigate reflood hydraulic behavior.

# PREFACE

EG&G Idaho, Inc., performs technical activities in the w reactor safety programs at the Idaho National Engineering Labora under the sponsorship of the U. S. Nuclear Regulatory Commissi Division of Reactor Safety Research. The current water reactor search activities of EG&G Idaho, Inc., are accomplished in the fo lowing programs: the Semiscale Program, the Loss-of-Fluid Test (LOFT) Experimental Program, the Thermal Fuels Behavior Program, the Code Development and Analysis Program, the Code Assessment and Applications Program, and the 3-D Experiment Project.

The Semiscale Program consists of a continuing series of small-scale nonnuclear thermal-hydraulic experiments having as their primary purpose the generation of experiment data that can be applied to the development and assessment of analytical models describing loss-of-coolant accident (LOCA) phenomena in water-cooled nuclear power plants. Emphasis is placed on acquiring system effects data from integral tests that characterize the most significant thermal-hydraulic phenomena likely to occur in the primary coolant system of a nuclear plant during the depressurization (blowdown) and emergency cooling phase of a LOCA. The Semiscale test facility is now in the Mod-3 test system configuration that contains two active loops and a full-length core and is scaled more directly to a pressurized water reactor (PWR) than was the former Mod-1 test system.

The LOFT Experimental Program is a nuclear test program for providing test data to support (a) assessment and improvement of the analytical methods utilized for predicting the behavior of a PWR under LOCA conditions, (b) evaluation of the performance of PWR engineered safety features, particularly the emergency core cooling system, and (c) assessment of the quantitative margins of safety inherent in the performance of these safety features. The test program utilizes the LOFT Facility, an extensively instrumented 55-MW pressurized water reactor facility designed for conduct of loss-of-coolant experiments (LOCEs). The test program includes a series of nonnuclear (without

nuclear heat) LOCEs followed by a series of low-power nuclear LOCEs and then a series of high-power nuclear LOCEs.

The Thermal Fuels Behavior Program is an integrated experimental and analytical program designed to provide information on the behavior of reactor fuels under normal, off-normal, and accident conditions. The experiment portion of the program is concentrated on testing of single fuel rods and fuel rod clusters under power-cooling-mismatch, loss-of-coolant, and reactivity initiated accident conditions. These tests provide in-pile experiment data for the evaluation and assessment of analytical models that are used to predict fuel behavior under reactor conditions spanning normal operation through severe hypothesized accidents. Data from this program provide a basis for improvement of the fuel models.

The earlier Reactor Behavior Program has been realigned as two programs dealing with code development and with code assessment. The Code Development and Analysis Program has the primary responsibility for the development of codes and analysis methods; it provides the analytical research aimed at predicting the response of nuclear power reactors under normal, off-normal, and accident conditions. The Code Assessment and Applications Program performs the task of assessing the accuracy and range of applicability of computer codes developed for the analysis of reactor behavior. The assessment process involves the analyses of many different experiments and the comparison of calculated results with experimental data. Statistical evaluations of both the analytical and experimental results are part of the assessment process.

The 3-D Experiment Project is a multinational cooperative water reactor research project which is intended to facilitate study of the behavior of entrained liquid in a full-scale upper plenum and cross flow in the core during the reflood phase of a PWR LOCA.

More detailed descriptions of the first four programs are presented in quarterly report for January through March 1975, ANCR-1245.

Later quarterly reports are ANCR-1262 (for April-June 1975), ANCR-1296 (for July-September 1975), ANCR-NUREG-1301 (for October-December 1975), ANCR-NUREG-1315 (for January-March 1976), TREE-NUREG-1004 (for April-June 1976), TREE NUREG-1017 (for July- September 1976), TREE-NUREG-1070 (for October-December 1976), TREE-NUREG-1128 (for January-March 1977), TREE-NUREG-1147 (for April-June 1977), TREE-NUREG-1188 (for July-September 1977), TREE-NUREG-1205 (for October-December 1977), TREE-NUREG-1218 (for January-March 1978), and TREE-1219 (for April-June 1978). Copies of the quarterly reports are available from the Technical Information Center, Department of Energy, Oak Ridge, Tennessee, and the National Technical Information Service, Springfield, Virginia.

## SUMMARY

Water reactor research activities performed by EG&G Idaho, Inc., at the Idaho National Engineering Laboratory during July through September 1978 are reported for the Semiscale Program, the LOFT Experimental Program, the Thermal Fuels Behavior Program, the Code Development and Analysis Program, the Code Assessment and Applications Program, and the 3-D Experiment Project.

For the Semiscale Program, four experiments in the baseline test series of the Semiscale Mod-3 system were conducted. Two of the experiments, Tests S-07-2 and S-07-3, were blowdown-refill experiments conducted from initial conditions (of pressure, temperature, and coolant flow) typical of PWR operating conditions. The third experiment, Test S-07-5, was a reflood test conducted to define thermal-hydraulic behavior of the system during the reflood phase of a 200% cold leg break in the Mod-3 system. Test S-07-6 was the first integral blowdown-reflood test conducted in the Mod-3 system. Test parameters for all four tests were within specified tolerances and test objectives were achieved. Atypical hydraulic behavior in the downcomer during Test S-07-6 resulted in delayed quenching of the core high power zone; further testing is required to ascertain the cause of the downcomer behavior. In Semiscale instrumentation development, application of a scanning densitometer system is described for measuring densities in steady two-phase flow and for indicating types of flow regimes that occur during the two-phase flow.

Results from LOFT nonnuclear Test Series L1, the first series of loss-of-coolant experiments (LOCEs) performed in LOFT, were evaluated to determine their relevance to licensing criteria for commercial pressurized water reactors. In general, the results support the conservative intent of those portions of the evaluation model requirements contained in the licensing criteria. The results are applicable to commercial reactors as was determined through validation of the scaling rationale for LOFT and Semiscale and assessment of current analytical models. The RELAP4/MOD6 (Version 4) computer code was used

in the predictive analysis for the first three tests in the first series of LOFT nuclear tests (Test Series L2). The calculated blowdown system response in the LOFT LOCEs was shown to be significantly different from the blowdown system response in the counterpart tests performed in Semiscale. The overall hydraulic reponse of LOFT is calculated to be very similar for the three LOFT LOCEs even though the power levels for the LOCEs differ substantially. A study was performed using the MOXY/SCORE computer code to evaluate the effect of cladding surface radiation heat transfer and three-dimensional core crossflow on LOFT loss-of-coolant accident behavior; results indicate that radiation heat losses for the higher power LOFT LOCEs will be significant and beneficial in reducing the maximum rod cladding temperature. Testing and calibration of LOFT mass flow measurement instruments in a flow test facility at Karlsruhe, Germany, were performed. Several different drag-disc turbine transducers were tested in small size pipes at steady state conditions; transducers tested included the type used in Test Series L1 and the newer modular drag disc currently being phased into the LOFT system. The gamma densitometer-drag disc was determined to be the best combination for determining mass flow rate.

The Thermal Fuels Behavior Program completed 20 driver core reactivity initiated accident (RIA) lead rod tests and 4 RIA Scoping Tests in the Power Burst Facility (PBF). The driver core lead rod tests consisted of nine-rod tests and nine-rod waterlogged-rod tests, which, together with the single-rod lead rod test conducted last quarter, constituted the burst mode PBF lead rod and core characteristics tests. The RIA scoping tests were the first tests ever conducted in which typical light water reactor fuel rods were subjected to a power burst at normal boiling water reactor system conditions. Other accomplishments included preparations for the LOFT Lead Rod Tests and Tests RIA 1-1, RIA 1-2, LOC-3, and GC 2-4 in the PBF; reporting of results from tests previously performed in the power-cooling-mismatch (PCM), loss-of-coolant accident (LOCA), and gap conductance (GC) test series; evaluation of the data from the long-term, steady state experiments being conducted in the Halden reactor; and examination of fuel

from commercial power reactors. Activities associated with planning anticipated transient without scram type tests in PBF indicated that pellet-cladding interaction, cladding ballooning rupture, and cladding oxidation are potential fuel failure mechanisms during BWR and PWR operational transients and during anticipated transient without scram events.

The Code Development and Analysis Program progressed in the development of the reference code RELAP4, the primary systems code RELAP5, the containment code BEACON/MOD2A, and an uncertainty analysis method for the fuel rod analysis code FRAP-T5. A best estimate fuel model was incorporated in the blowdown version of RELAP4/MOD7 V2. Application of RELAP5 to the calculation of a Semiscale Mod-1 isothermal blowdown test was completed. A wall heat transfer capability was incorporated into the BEACON/MOD2A code. In fuel rod modeling, an uncertainty anal; s procedure was incorporated in FRAP-T5 to facilitate determination of the effects of various fuel rod input uncertainties on calculated fuel rod behavior.

The Code Assessment and Applications Program continued assessment of the thermal-hydraulic code RELAP4/MOD6, completed assessment of the fuel rod analysis code FRAP-T4 and prepared for assessing FRAPCON 1. Participation in NRC-industry programs was continued. A jet pump testing effort associated with the boiling water reactor-blowdown/emergency core cooling area of the NRC-industry program was completed. Calculations of performance were made for a steam generator reference test associated with the FLECHT-SEASET Program. Development and expansion of the NRC/RSR data bank were continued.

The 3-D Experiment Project continued the development of specialized two-phase fluid measurement instruments (instrumented flow sections, liquid level detectors, turbine flow meters, and drag discs) for safety experiments in Germany and Japan. Testing and preliminary analysis of the 3-D Air-Water Upper Plenum Test Program were completed.

CONTENTS

FIGURES

TABLES

# QUARTERLY TECHNICAL PROGRESS REPORT ON WATER REACTOR SAFETY PROGRAMS SPONSORED BY THE NUCLEAR REGULATORY COMMISSION'S DIVISION OF REACTOR SAFETY RESEARCH JULY-SEPTEMBER 1978

## I. SEMISCALE PROGRAM

D. J. Olson, Manager

Four tests were performed with the Semiscale Mod-3 system during the quarter, and preliminary assessment of results indicates that test objectives were accomplished. Two experiment data reports[1,2] were published for the first two tests conducted with the Mod-3 system, Tests S-07-1 and S-07-4. These tests were conducted in June 1978 and were briefly reported in the quarterly report for April-June 1978[3].

Evaluation of a scanning densitometer system is presented with regard to its application for measuring densities in two-phase flow and for indicating types of flow regimes that occur during the two-phase flow phenomena in loss-of-coolant experiments.

### 1. SEMISCALE MOD-3 TESTING

Four experiments in the baseline test series (Test Series 7) for the Semiscale Mod-3 system were conducted. Two of the four experiments were blowdown-refill experiments conducted from initial conditions (pressure, temperature, and coolant flow) that are typical of PWR operating conditions. One of the experiments was a reflood test and one was an integral blowdown-reflood test. Objectives of the first experiment, Test S-07-2, were to assess the effect of radial power peaking on core thermal-hydraulic behavior and to evaluate the effect of emergency core coolant (ECC) subcooling on downcomer penetration characteristics. The objectives of the second blowdown-refill experiment, Test S-07-3, were to assess the effects of (a) containment pressure at the end of blowdown conditions and (b) locating the system pressurizer in the broken loop hot leg rather than in the intact loop hot leg.

The third experiment, Test S-07-5, was a reflood test performed with the objectives of (a) defining the thermal-hydraulic behavior under reflood conditions representative of an integral 200% cold leg break in the Mod-3 system, (b) providing insight into the effect of initial conditions on reflood behavior, (c) providing information on downcomer and upper plenum hydraulic behavior, and (d) providing data for code evaluation.

Preliminary evaluation of the data from Tests S-07-2, S-07-3, and S-07-5 indicates that the important test parameters were within specified tolerances and that the objectives were achieved.

Test S-07-6, the fourth experiment performed during the quarter, was the first integral blowdown-reflood test conducted in the Mod-3 system. The principal objective of Test S-07-6 was to provide reference data for a 200% cold leg break test which would permit an evaluation of the Mod-3 integral blowdown-reflood behavior and would provide insight into expected system operating characteristics. Preliminary evaluation of the data from Test S-07-6 indicates that initial conditions and test parameters were within the specified tolerances. However, the test exhibited downcomer hydraulic behavior which resulted in delaying quenching of the core high power zone until about 550 seconds after rupture. The downcomer fluid behavior exhibited in Test S-07-6 is considered to be not typical of the behavior which may occur in a PWR system; however, further testing will be required to identify the exact causes of the downcomer fluid behavior in the Mod-3 system.

## 2. APPLICATION OF A SCANNING DENSITOMETER FOR INDICATING FLOW REGIMES DURING TWO-PHASE FLOW

A. G. Stephens

One of the principal comparison points or areas of interest for water reactor safety code development and assessment and loss-of-coolant experiments is the two-phase mass flow rate at various times and flow area locations within an experimental system. Two variables, density and velocity, must be measured to determine mass flow rate. In

single-phase conditions, and for which the phase is all-liquid or all-vapor, the density can be determined from pressure and temperature measurements, and the variation of density over the flow cross section is usually negligible. Under such conditions, measurements obtained from an orifice, venturi, or turbine flowmeter together with the pressure and temperature give the mass flow rate. However, in two-phase mixtures, the density is different at different places in the flow cross section, and the density variation may be large, covering the full range from liquid to vapor values. The pressure or temperature or both establish the limits of this variation, but not the required density versus space and time relation. A separate instrument, the multibeam densitometer, is used to obtain the density data. Either, or both, of two other instruments is used to determine the velocity: a turbine flowmeter for velocity directly, or a drag device for momentum flux which, with the density, can give velocity. (Recent development of a full-flow drag device was reported in Reference 4, pp. 3-9).

Two- and three-beam densitometers based on the photon attenuation technique are used by EG&G Idaho, Inc. In using this technique, the time variation in the count rate of transmitted (detected) photons is related to the time variation of length-averaged fluid density along the beam or sight line from a radiation source through a pipe and fluid to the detector. These nonintrusive measuring systems are particularly well suited to a system-effects test facility such as Semiscale, since such a facility has a lower tolerance to measuring-instrument-induced flow disturbances than would a separate-effects test facility.

As with many two-phase measurement techniques, applications problems are encountered in integrating the measurement concept with the system. Presently, the most difficult and important problem concerns the conversion of the count rate data to information which can be used with the velocity or momentum flux data to calculate mass flow rate. In Semiscale the chordal average density data are converted to a cross-sectional average density. The type of flow must be known to make this conversion when the interrogated area (which is the sum of the beam

areas) is a fraction of the total flow area. That is, a mathematical model must be used which describes the local density variation over the flow and which can be used to relate chordal and cross-sectional average density values. Flow regime determination, either by the density measuring system or some other instrument, is necessary for a successful cross-sectional average density calculation when the interrogated area is only a fraction of the total. To verify the correctness of a densitometer measurement and data reduction calculation, a reference densitometer must be provided which gives both an accurate measurement of the cross-sectional average density and one which also gives, unequivocally, the type of flow regime observed.

A reference densitometer having the requisite capabilities of providing an accurate cross-sectional average density and a reliable indication of the type of flow regime was designed and constructed at the Semiscale air-water test facility. It consisted of a scanning or traversing detector, a fixed position X-ray source, and a piping spool piece (or flow spool) on which the detector and source were mounted. A diagram of the arrangement is shown in Figure 1. A traversing scheme was chosen on the basis of earlier work at Argonne National Laboratory[5], the University of Minnesota[6], and by others[7,8] showing the advantages of this method over that of the single stationary beam. The technique used was similar to that used earlier by the author[9,10] and is characterized by a fixed source, a small exposed detector area, and a traversing mechanism to move the detector in an arc about the source point (as shown in Figure 1) to obtain data at many chordal positions over the flow field. The detector was a liquid-nitrogen-cooled silicon semiconductor having excellent photon energy resolution. The use of a low-energy characteristic X-ray emitting source (cadmium-109) was facilitated by incorporation of a beryllium ring between a pair of flanges in the pipe spool piece. The 22 keV X-rays provided near optimum densitometer sensitivity in the 66.7-mm diameter flow area of the piping spool piece. The beryllium pressure containing ring permits use of such low-energy photons because the ring attenuates them even less than does the contained liquid. This arrangement also provides improved capability to distinguish between flow

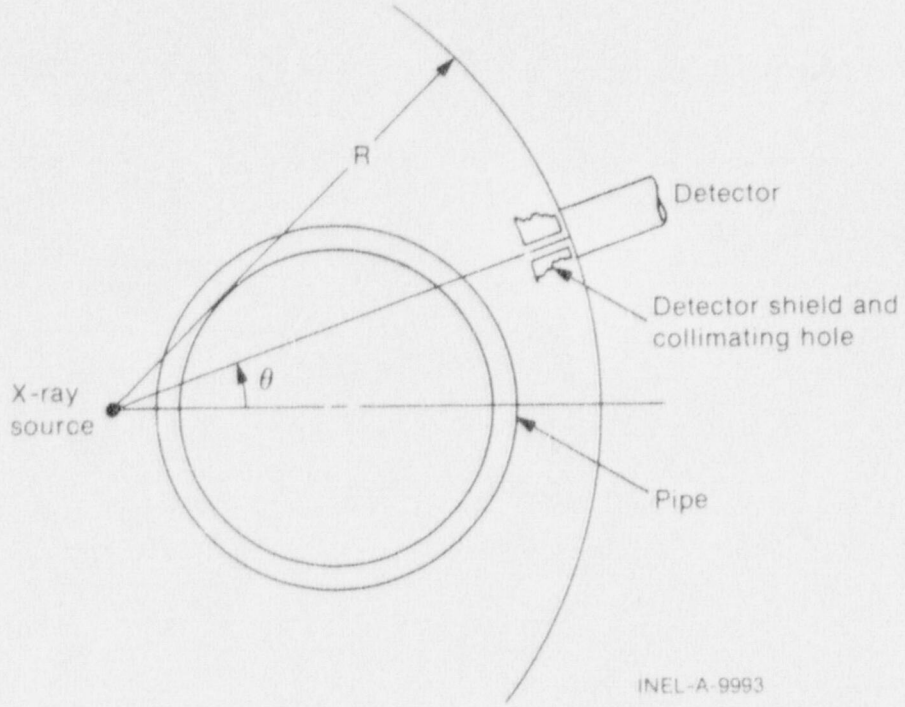


Fig. 1 Scanning densitometer arrangement showing X-ray source, cross section of piping spool piece, and angle $\theta$ which defines the location of traversing detector.

regimes by means of the shape of traverse count rate and chordal average density data.

Figure 2 shows scanning densitometer data taken in the air-water loop at various air superficial velocities that are expected to yield annular flow regime conditions, and Figure 3 shows similar data (in terms of X-ray count rates) for various vapor superficial velocities that are expected to indicate stratified flow regimes. In Figure 2, values of chordal average density are plotted for each detector position. These density values are calculated from detected X-ray count rates using Equation (1).

$$\rho_c(\theta) = \rho_f - (\rho_f - \rho_g) \frac{\left(\ln \frac{I(\theta)}{I_f(\theta)}\right)}{\left(\ln \frac{I_g(\theta)}{I_f(\theta)}\right)} \qquad (1)$$

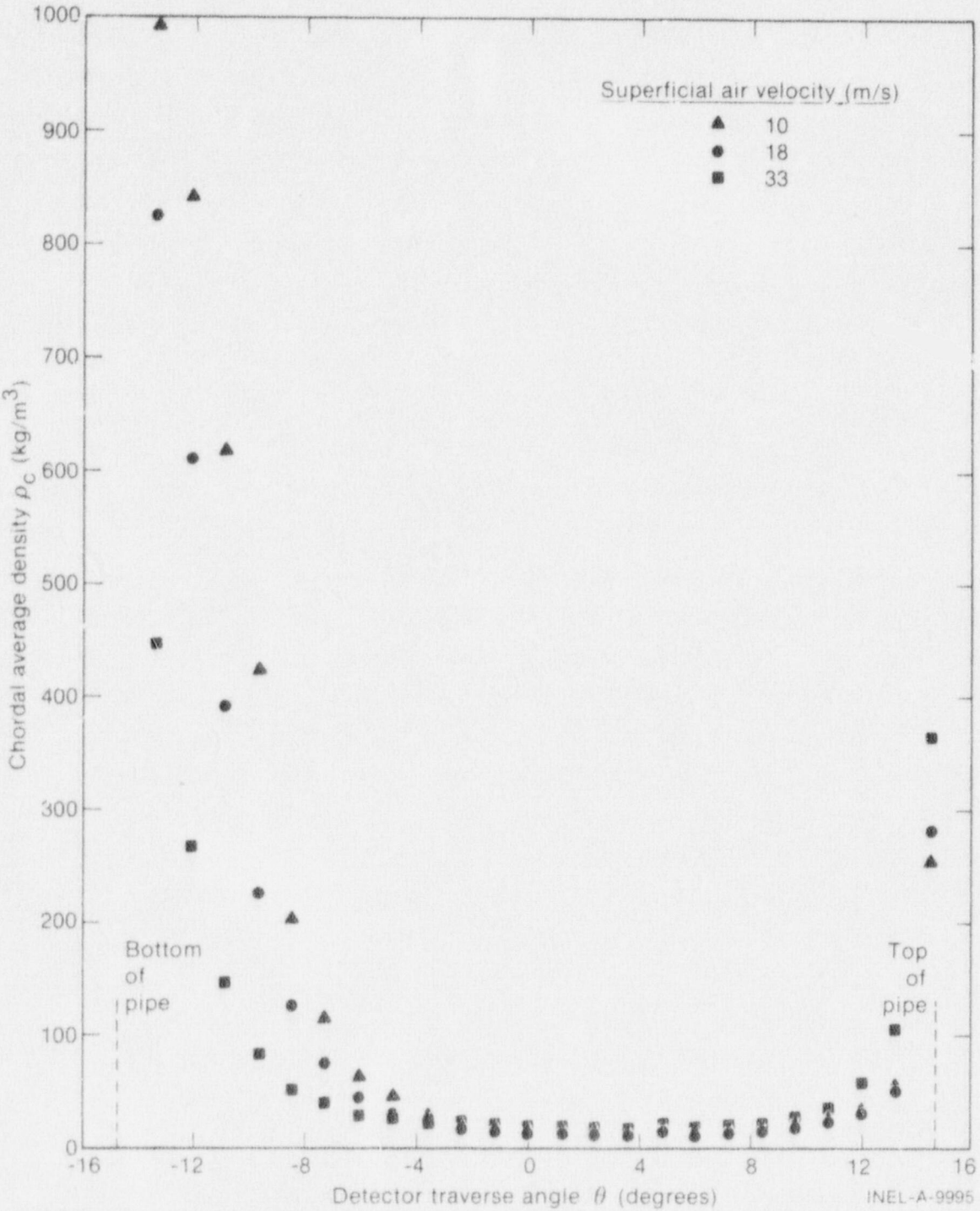


Fig. 2 Average fluid densities (calculated from X-ray count rates) at different locations (angle $\theta$) across pipe at constant water superficial velocity of 0.1 m/s and at various air superficial velocities. Density patterns indicate annular flow regimes.

where

$\rho_c(\theta)$ = chordal average two-phase mixture density at detector position $\theta$

$I_f(\theta)$ = X-ray count rate at $\theta$ for all-liquid condition in pipe

$I_g(\theta)$ = X-ray count rate at $\theta$ for all-vapor pipe condition

$I(\theta)$ = X-ray count rate at $\theta$ for two-phase condition

$\rho_f$ = density of liquid giving $I_f$ count rates

$\rho_g$ = density of vapor giving $I_g$ count rates.

In Figure 3, actual count rate data are plotted for the various detector positions.

The data in Figure 2 show the expected low densities in a central core and higher densities at the pipe top and bottom. The core is seen to be eccentric to the horizontal pipe (thicker annulus at bottom) and essentially homogeneous (constant density) over most of its central part. The density in the annulus is less than that of water, indicating a significant concentration of entrained air. The three different flow conditions show the effects of varying air flow at constant water flow: with increasing air flow, the core becomes more concentric with the pipe and larger in diameter. These conditions imply a thinner annulus near pipe mid-height which, in the face of the constancy of the chordal average densities there, implies an increased concentration of entrained liquid. This interpretation is consistent with the simple intuitive result that an increased air velocity should increase the average water velocity.

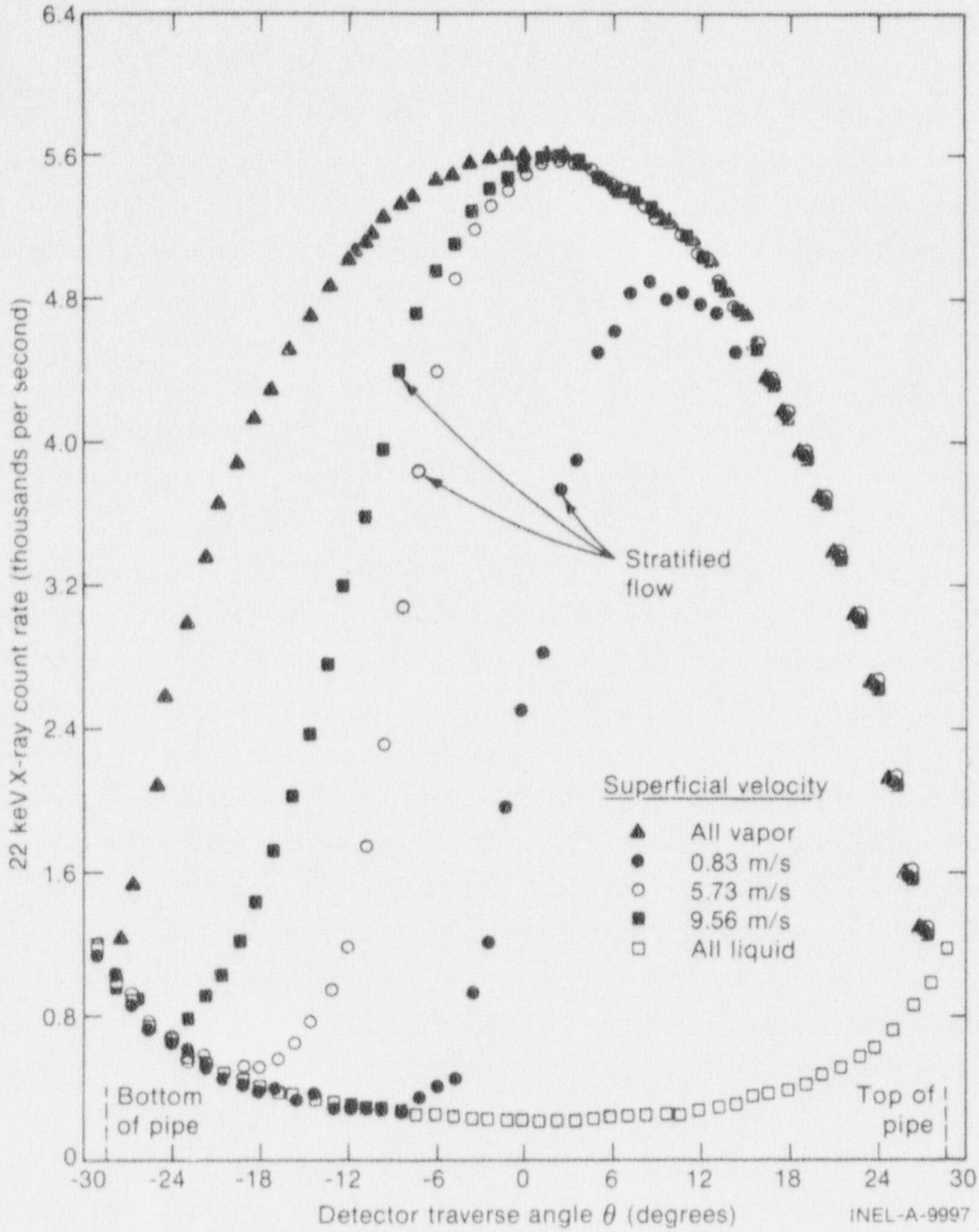


Fig. 3 X-ray count rates at different locations (angle $\theta$) for constant water superficial velocity of 0.51 m/s and at various vapor superficial velocities. Stratified flow regimes are indicated between the all-vapor and all-liquid flow regimes.

In Figure 3, the all-vapor and all-liquid data from the traverses of the scanning densitometer are plotted in addition to the three stratified flow conditions. The shape of the all-vapor traverse is due to the variation of pipe wall thickness with detector traverse angle: the metal thickness is least for a diametral beam, and thus the highest

transmitted and detected count rate occurs at  = 0. In lower sensitivity experiments, the shape of the all-liquid traverse would also be concave downward, but because the beryllium is so transparent, the shape of the all-liquid traverse is due to the variation of liquid thickness with traverse angle. Thus at a diameter at which  = 0 the liquid thickness is greatest and the detected count rate least.

The three stratified flow variations in Figure 3 show again the effects of increasing vapor flow at constant liquid flow, but at lower values of each. As the vapor flow increases, the basically horizontal interfacial zone expands downward. The increased vapor flow tends to entrain the uppermost liquid layers, thus enlarging the interfacial zone, decreasing the area of unaffected liquid, and increasing the vapor area.

Thus, as can be seen in Figures 2 and 3, the scanning densitometer can provide the needed flow regime information. In addition, because the full flow area is covered in the traverse, the cross-sectional average density can be calculated directly, weighting each chordal average density value with the appropriate beam area.

Finally, Figure 4 shows how the scanning densitometer is used to verify the correctness of a multibeam densitometer data reduction model. Multibeam and scanning densitometers were mounted side by side and used to monitor a stratified flow regime. Three chordal average density readings were obtained, one from each of the three beams of the multibeam densitometer. Forty-seven chordal average density values were obtained by the scanning densitometer monitoring the same flow. The scanning densitometer data are plotted in Figure 4. The three values from the multibeam densitometer and the information that the flow regime was stratified were used in Lassahn's stratified three-beam densitometer data reduction model[11]. The output from that model is the other density distribution shown in Figure 4.

The good agreement between the scanning densitometer data distribution and that calculated from the multibeam densitometer data gives a

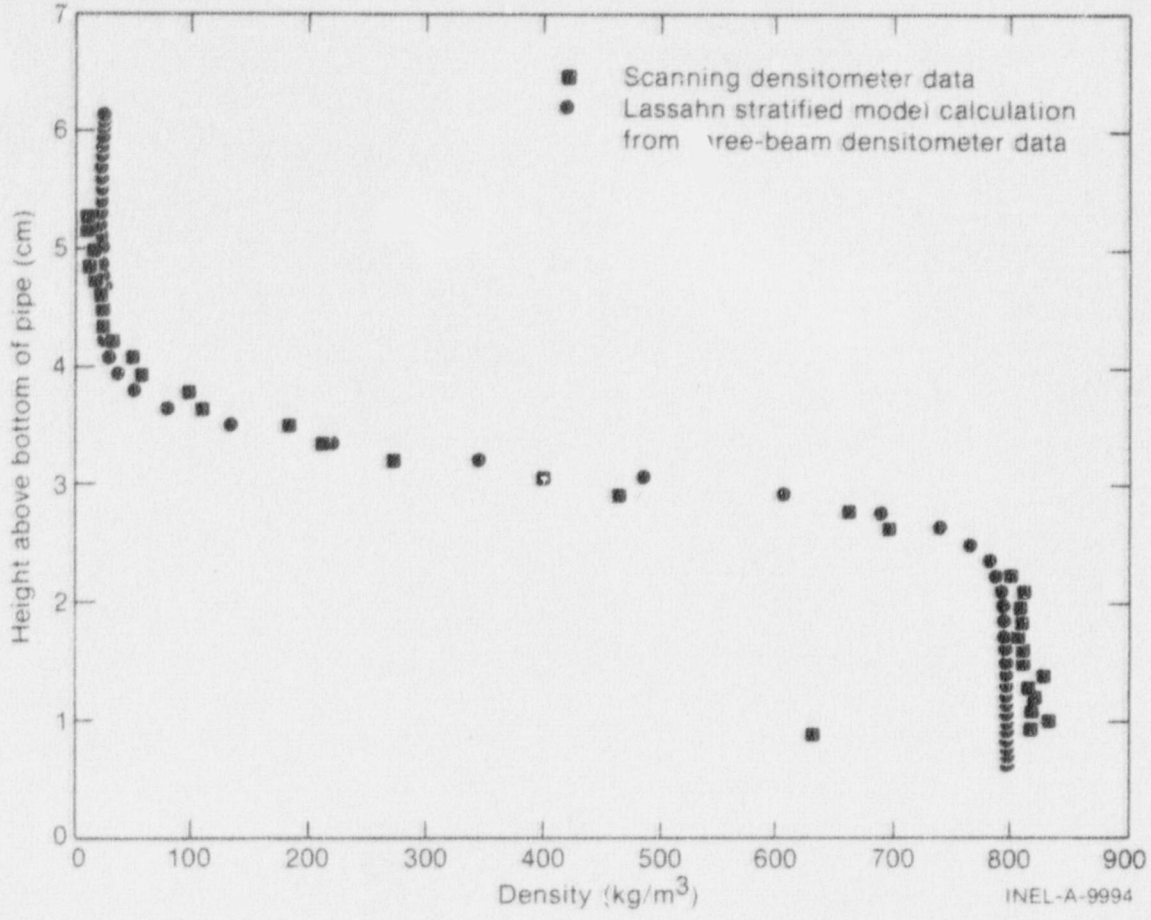


Fig. 4 Comparison of densities from scanning densitometer data with densities calculated using Lassahn stratified model and three-beam densitometer data.

high level of confidence in the multibeam densitometer data reduction model. Although this result is encouraging, in practical application the appropriate type of flow regime must still be determined in order to apply the appropriate data reduction model to the multibeam densitometer data.

In summary, the objective of providing accurate indication of cross-sectional average density and reliable indication of the type of flow regime was accomplished: a scanning densitometer was constructed and is being used as a reference densitometer to provide flow regime and cross-sectional average density information for the purpose of verifying the measurement accuracy and the validity of the data reduction model for multibeam densitometer measurements.

# II. LOFT EXPERIMENTAL PROGRAM

L. P. Leach, Manager

The LOFT Program has been developed to provide experimental information relevant to the licensing criteria for pressurized water reactors (PWRs). The major portion of the program is directed at achieving improved understanding of the loss-of-coolant accident (LOCA) and the performance of emergency core cooling systems through analysis of the phenomena associated with such accidents observed in planned loss-of-coolant experiments (LOCEs). The first series of experiments, a nonnuclear test series designated Test Series L1, has been completed. Significant results obtained from Test Series L1 are summarized in Section 1.

Preparations for the first series of nuclear tests (Test Series L2, Power Ascension Test Series) are in progress. Nuclear power range testing of the LOFT reactor is nearly completed. The analytical work for the predictive analysis for the first three tests in the series (LOCEs L2-2, L2-3, and L2-4) has been completed. A brief discussion of the significant results from the system depressurization calculations for LOCEs L2-2, L2-3, and L2-4 is presented in Section 2. The potential influence of three-dimensional core coolant behavior and radiation heat transfer on peak temperature of the fuel rod cladding during the blowdown phase of a LOCE was evaluated in a preliminary study. The results of this study are summarized in Section 3.

The instruments to measure mass flow in LOFT during the LOCEs were tested and calibrated in a flow test facility at Karlsruhe, Germany. Conclusions from the Karlsruhe testing are presented in Section 4.

## 1. SUMMARY OF SALIENT RESULTS FROM LOFT NONNUCLEAR TEST SERIES L1

V. T. Berta

Significant results obtained from Test Series L1 concerning blowdown thermal-hydraulics and structural phenomena are summarized. Test

Series L1 included variations in principal parameters associated with break size and location, ECC injection, and primary system component operation. The framework for this discussion is the two fundamental aspects of the LOFT Program objectives: (a) the validation of the scaling rationale and (b) the validation of the analytical models intended for commercial PWR application.

## 1.1 Assessment of the Scaling Rationale

The assessment of scaling rationale from Test Series L1 results is summarized as follows:

(1) Intact loop resistance has no significant effect on the thermal-hydraulics in a LOCA. Both Semiscale and LOFT experimental data show insignificant intact loop resistance effects on blowdown thermal-hydraulics.

(2) ECC delivery delay to the lower plenum (hot-wall delay) in commercial PWRs will be no greater than that in LOFT (0.5 to 1.0 s) and thus would not be a significant deterrent to operation of the emergency core coolant system.

(3) ECC bypass in commercial PWRs at the time the accumulators empty will be less than (or no greater than) that in LOFT ($\simeq$30%).

(4) ECC mixing with primary coolant is not instantaneous and does not cause significant pressure oscillations. The coolant temperature in the LOFT lower plenum is as much as 50 K below saturation which should be near the limit in commercial PWRs since the ECC flow path to the lower plenum is somewhat longer and provides more time for mixing.

(5) LOFT Test Series L1 experiments and Semiscale counterpart experiments show incomplete voiding of the lower plenum. The observed trends indicate that incomplete voiding will also occur in the lower plenum of commercial PWRs.

(6) Accumulator nitrogen expansion, inversely dependent on the surface-to-volume ratio, is nearly isentropic in LOFT (the polytropic gas constant n = 1.3) and is expected to be very near isentropic in PWR accumulators (n = 1.37).

(7) Primary coolant pump operational variations do not affect significantly the hot wall delay, ECC bypass, or lower plenum voiding.

## 1.2 Analytical Model Comparisons with LOFT Data

The assessment of the analytical model comparisons is summarized as follows:

(1) RELAP4 computer code[12] calculations are in good agreement with Test Series L1 experimental results where one-dimensional, homogeneous equilibrium assumptions are valid.

(2) Observed multi-dimensional or asymmetric flow in the downcomer is best calculated with models that permit such flow. However, one-dimensional modeling of the downcomer is in keeping with the conservative intent of evaluation models.

(3) Observed nonhomogeneous and incomplete ECC mixing in LOFT has resulted in the development of a noninstantaneous mixing model for inclusion in the RELAP4 code.

(4) Subcooled blowdown and structural load analysis techniques currently used in PWR design provide large safety factors in LOFT. Such practices in PWR design are expected to result in a structurally sound system in the event of a LOCA.

(5) Relatively accurate modeling has been achieved for pump flow, break flow, and pressurizer flow. The Semiscale pump degradation model works well for LOFT and may be satisfactory for commercial PWRs. Pressurizer flow models must include all the important pressure loss phenomena in the surge line.

## 2. EXPERIMENT PREDICTIONS FOR FIRST SERIES OF LOFT NUCLEAR TESTS

W. H. Grush

The first three LOCEs (LOCEs L2-2, L2-3, and L2-4) of LOFT Test Series L2, Power Ascension Test Series, will simulate double-ended offset shear breaks in the cold leg of the primary coolant system. ECC will be injected into the intact loop cold leg. The LOCEs will differ mainly in the power levels. The significant features of the analytical results of the RELAP4/MOD6[a] blowdown calculations for LOCEs L2-2, L2-3, and L2-4 are discussed.

### 2.1 Blowdown System Analytical Results

The pressure responses of the primary system as calculated for the first three LOFT LOCEs in Test Series L2 and as measured in three Semiscale experiments are compared in Figure 5. The Semiscale tests used in the comparison (Tests S-06-2, S-06-3, and S-06-4) are counterpart experiments to LOFT LOCEs L2-2, L2-3, and L2-4, respectively. Although the LOFT and Semiscale depressurizations are shown to have the

[a] RELAP4/MOD6, Update 4: EG&G Idaho, Inc., Configuration Control Number H00286IB.

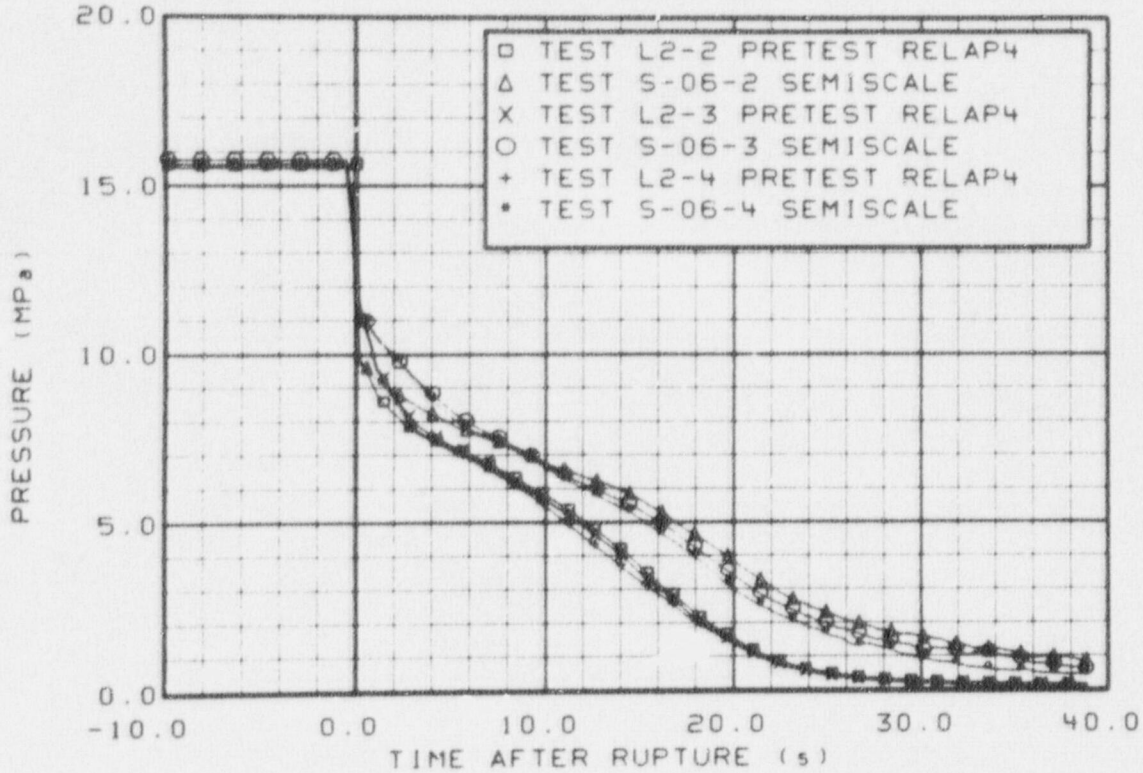


Fig. 5 Comparison of primary system pressure responses calculated for three LOFT LOCEs and measured data from counterpart tests conducted in Semiscale.

same shapes, the LOFT system is predicted to depressurize faster than the Semiscale system. The predicted difference in primary system depressurizations between LOFT and Semiscale is attributed to scaling differences. The Semiscale system has approximately 34% more fluid in the intact loop hot leg and upper plenum than if it were ideally volume scaled to LOFT. The presence of more high-temperature fluid i these Semiscale volumes is expected to be the major cause of the early departure between the LOFT-calculated and Semiscale measured primary system pressure responses.

The calculated pressure responses are similar for all three LOFT LOCEs transients. The lower initial pressure for LOCE L2-2 in the 0.1-to-3-second time period is attributed to the fact that the intact loop hot leg and upper plenum fluid temperature is 11 K lower for LOCE L2-2 than for LOCEs L2-3 and L2-4.

Comparison between the RELAP4 calculations for LOFT and the data from the Semiscale counterpart test , in general, indicates that the LOFT and Semiscale systems have significant differences in the overall hydraulic response during blowdown. The calculated behavior for LOCEs L2-2, L2-3, and L2-4 is very similar.

The calculated lower plenum liquid levels for LOCEs L2-2, L2-3, and L2-4 are compared in Figure 6. The behavior is similar for all three LOCEs. Reflood is calculated to begin at approximately 38 seconds after blowdown initiation for all three transients.

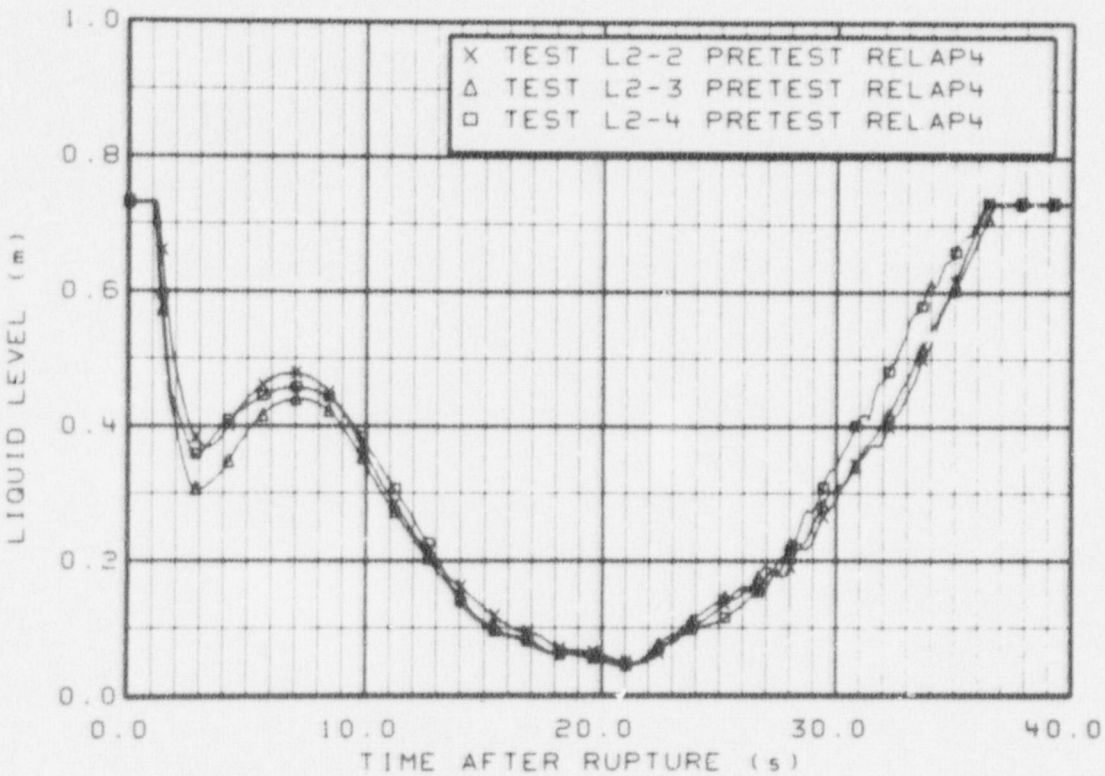


Fig. 6 Comparison of liquid levels in lower plenum calculated with RELAP4/MOD6 for LOFT LOCEs L2-2, L2-3, and L2-4.

## 2.2 Conclusions

The blowdown system analysis indicates that significant differences in system response are predicted to occur in the three LOFT LOCEs as compared with the measured data from the LOFT counterpart tests conducted in the Semiscale system.

The overall hydraulic response of LOFT is calculated to be very similar for LOFT LOCEs L2-2, L2-3, and L2-4, even though the power levels at which these LOCEs are conducted differ substantially. This trend, if correctly predicted by the code, may be useful in planning future LOFT experiments.

## 3. POTENTIAL INFLUENCE OF CROSSFLOW AND RADIATION HEAT TRANSFER ON LOFT LOCA BEHAVIOR

S. Chang and E. L. Tolman

The current prediction procedure for LOFT Test Series L2 utilizes one-dimensional analytical codes, as discussed in Section 2. The potential influence of three-dimensional core coolant behavior and radiation heat transfer on peak cladding temperature during the blowdown phase of a LOFT LOCE was evaluated in a preliminary study.

LOFT LOCE L2-4, which will have a maximum linear heat generation rate of 52.5 kW/m (the maximum LOFT operating power), was selected as the reference case for the LOCE analysis because it will have the most severe core thermal-hydraulic response of any LOCE in Test Series L2. The MOXY/SCORE code[a] was utilized for this study because the code has a three-dimensional hydrodynamic capability, a fuel rod model for temperature calculations, and a radiation heat transfer capability.

To evaluate the effect of cladding surface radiation heat transfer and three-dimensional core crossflow, the following cases were analyzed and compared:

(1) Three-dimensional MOXY/SCORE calculations with radiation heat transfer

(2) Three-dimensional MOXY/SCORE calculations with radiation heat transfer suppressed

---

[a] MOXY/SCORE, Version 4: EG&G Idaho, Inc., Configuration Control Number H00147IB.

(3) One-dimensional MOXY/SCORE calculations for the core hot rod.

The three-dimensional LOFT core was represented in MOXY/SCORE as one of four symmetric (quarter core) regions. The quarter core region was divided radially into 16 subchannels with 15 axial levels in each. The coolant boundary conditions (inlet axial velocity, inlet internal energy, and outlet internal energy and pressure) were taken from RELAP4/MOD5 system calculations and were assumed to be uniform over the core lower and upper boundaries.

The maximum rod cladding temperatures for each of the cases considered are shown in Figure 7. Radiation heat transfer during blowdown is shown to reduce the maximum cladding temperature by 100 K. Core crossflow, as a result of the core power gradient, reduces the calculated maximum cladding temperature by an additional 25 K. The maximum

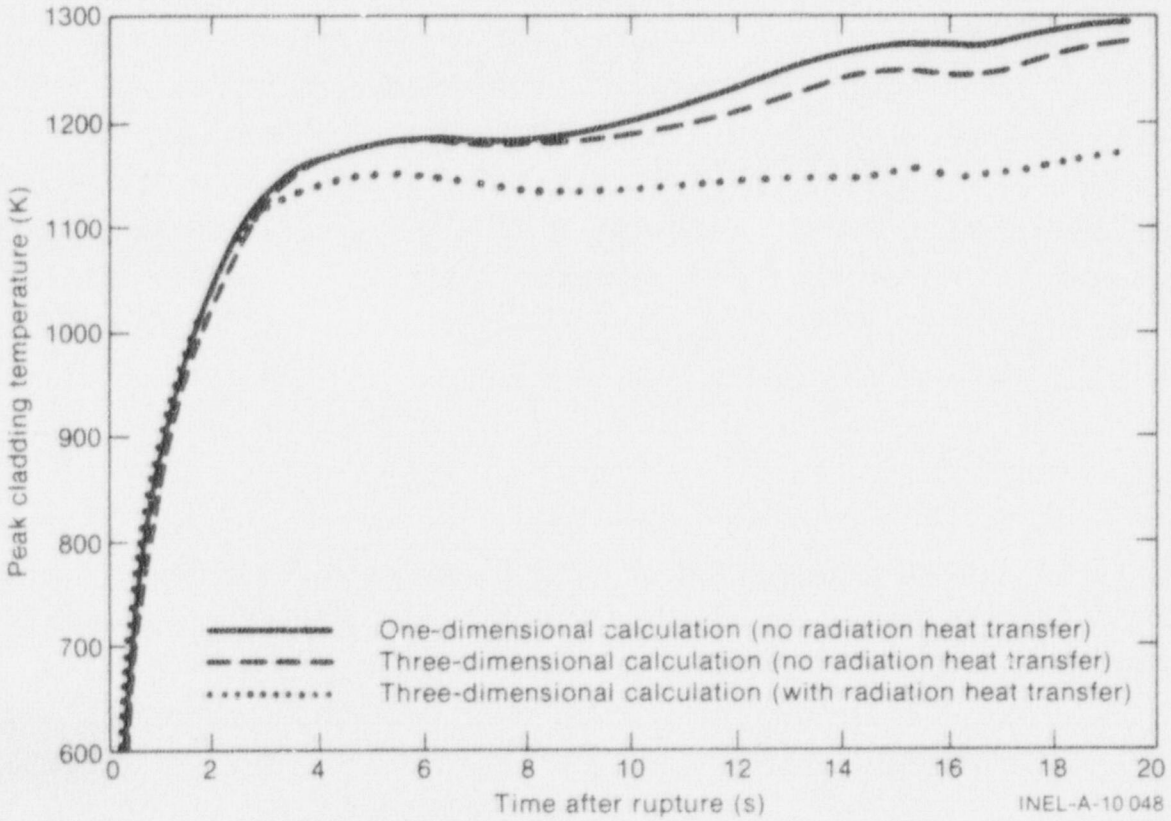


Fig. 7 Results of maximum cladding temperature calculations for LOFT LOCE L2-4 using MOXY/SCORE computer code.

cladding temperatures are somewhat lower than the best estimate predictions because of differences in the fuel thermal models. More accurate fuel thermal models are currently being programmed into MOXY/SCORE.

The results indicate that radiation heat losses for the higher power LOFT tests will be significant and beneficial in reducing the maximum cladding temperature.

## 4. CALIBRATION OF LOFT MASS FLOW INSTRUMENTS

C. W. Solbrig

A cooperative program was conducted with the nuclear research center (Kernforschungzentrum) in Karlsruhe, Germany, to test and calibrate mass flow measurement instruments in small size pipes with steady state flow. The objectives of this work were to: (a) provide calibration data in horizontal two-phase steady state flow to determine which of the commonly used methods of calculating mass flow is the best, (b) determine the usefulness of air-water calibration data, (c) provide a future instrument correlation data base, (d) correlate gamma densitometer readings to flow regime, and (e) determine pipe size, pressure, and vapor fraction effects on instrument calibration.

The instruments that were tested included the LOFT drag-disc turbine transducer (DTT) and a LOFT-type gamma densitometer. Several different DTTs were tested including the type used in the Test Series L1 LOCEs and the newer modular DTTs currently being phased into the LOFT system. Testing was accomplished in 3-inch Schedule 160 pipe and 5-inch Schedule 160 pipe test sections. Data were obtained in air-water as well as steam-water. Different pressures were investigated. Reference mass flow measurements were provided by orifice measurements in single-phase flow measured upstream of the mixing section. Two advanced reference instruments were included in this test series: an impedance probe for measuring the distribution of steam fraction in the vertical direction and the radiotracer (radioactive tracer detector) for measuring the velocity of each phase.

The mass velocity (mass flow per unit area) can be calculated by at least three methods with the drag disc, the turbine flowmeter, and the gamma densitometer. Figure 8 compares between the mass velocity as calculated from the combination of the gamma densitometer and turbine flowmeter versus the reference mass velocity. The scatter of these data is quite large, although parametric studies of these data show that they follow smooth parametric trends. Figure 9 shows a plot of the mass velocity as calculated by the gamma densitometer and drag-disc combination. These data, even though they are for the same flows as shown in Figure 8, show much better correlation with the reference mass

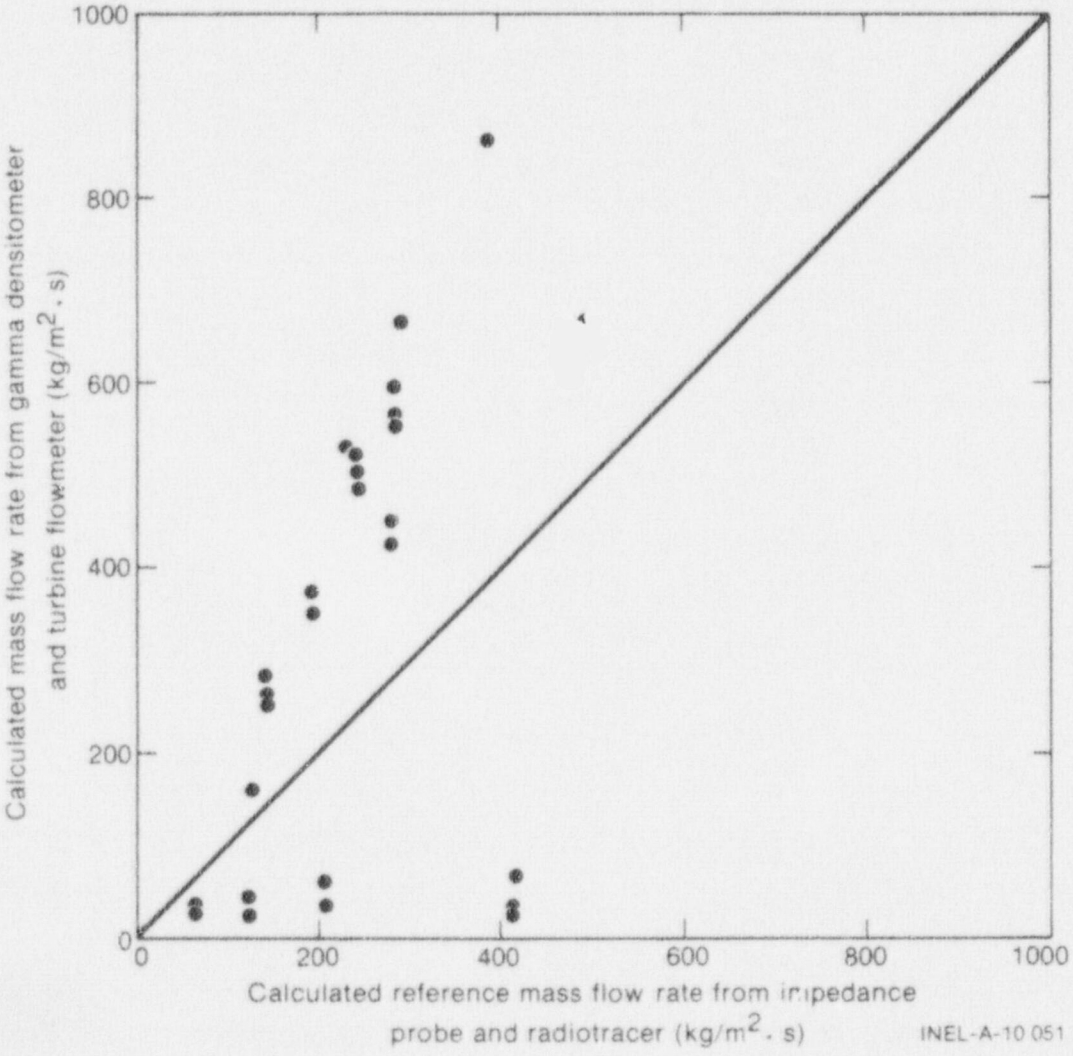


Fig. 8 Comparison of mass velocities as calculated from the gamma densitometer and turbine flowmeter versus the reference impedance probe and radiotracer.

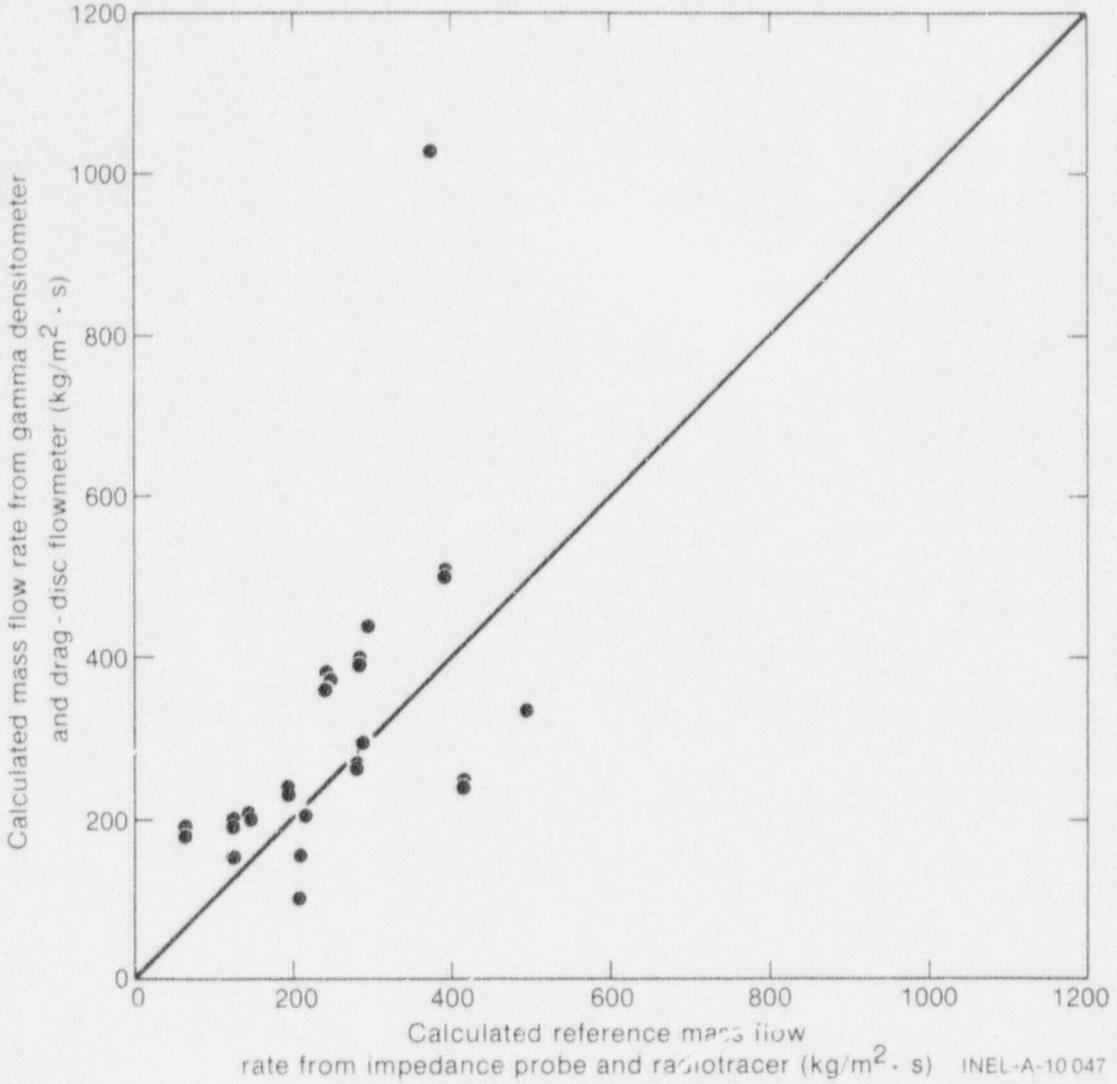


Fig. 9 Comparison of mass velocities as calculated from the gamma densitometer and drag-disc flowmeter versus the impedance probe and radiotracer.

flow measurements. The root mean square error for the gamma densitometer drag-disc combination is significantly less than the errors of the other two methods.

Conclusions from these tests are that: (a) the gamma densitometer and drag disc is the better combination for determining mass flow rate; (b) the inaccuracy of mass flow measurement increases with void fraction, air-water data are not especially accurate, and the accuracy can be increased considerably if the slip is known; (c) the modular drag unit performs much better than the drag disc used in LOFT Test Series

L1; and (d) the new models which have been developed determine the mass flow much better than the previous methods.

The LOFT Program has obtained the radiotracer and impedance probe as new technologies for reference measurements.

# III. THERMAL FUELS BEHAVIOR PROGRAM

H. J. Zeile, Manager

The Thermal Fuels Behavior Program (TFBP) completed 20 driver core reactivity initiated accident (RIA) lead rod tests and four RIA Scoping Tests in the Power Burst Facility (PBF). The RIA Scoping Tests were the first tests ever conducted in which typical light water reactor fuel rods were subjected to a power burst at normal boiling water reactor system conditions. Other accomplishments included preparations for the RIA 1-1, RIA 1-2, LOFT lead rod, LOC-3, and GC 2-4 tests in the PBF; reporting of results obtained from tests previously performed in the Power-Cooling-Mismatch (PCM), Loss-of-Coolant Accident (LOCA), and Gap Conductance (GC) Test Series in PBF; evaluation of the data from the long term, steady state experiments being conducted in the Halden reactor; and examination of fuel from commercial power reactors.

The following sections describe (a) PBF testing and (b) activities in the area of program development, data analysis, Halden fuel behavior research, postirradiation examination of commercial power reactor fuel, Nuclear Regulatory Commission technical assistance, and coordination with foreign experimental programs.

## 1. PBF TESTING

P. E. MacDonald and R. K. McCardell

Tests in the PBF this quarter included (a) 20 driver core RIA lead rod tests and (b) the RIA Scoping Test Series which consisted of four single-rod tests using typical light water reactor fuel.

### 1.1 Lead Rod Testing

R. L. Benedetti

The PBF lead-rod and core characteristics tests were completed using nine-rod clusters containing both intact and waterlogged PBF driver core fuel rods in the PBF in-pile tube. Because of the large volume of moderator in the in-pile tube, selected PBF driver core rods

were subjected to relatively high power conditions while the driver core itself remained at modest power.

1.1.1 Nine-Rod Lead Rod Test. With completion of the nine-rod lead rod test the PBF fuel rods have been subjected to peak fuel enthalpies up to 8033 J/cm$^3$, which is equivalent to a core energy release of 1280 MJ. The PBF core has been qualified to 670-MJ burst energy release and a 2.01-ms reactor period (maximum programmatic requirement is about 700 MJ). The natural burst axial growth behavior of PBF fuel rods that have been previously exposed to long periods of high power operation and fuel centerline melting was measured at a peak fuel enthalpy of 6694 J/cm$^3$. Appropriate core kinetic behavior data have been obtained which verify physics predictions of the PBF core power response. During the nine-rod lead rod test, a total of 36 power bursts were run.

Preliminary assessment of the data from the nine-rod tests indicated that long periods of high power steady state operation and centerline melting are not detrimental to to the natural burst mode lifetime of PBF rods. However, posttest examination revealed that all nine rods in the cluster exhibited a wavy deformation on the lower 35.6 cm. The physical phenomena which caused the deformation have not been determined. Neutron radiographs are being made, and a comparison will be made between the nine-rod lead rod results and those from previous capsule driver core (CDC) tests.

1.1.2 Nine-Rod Waterlogged Test. The objective of the waterlogged rod test was to determine whether the failure of a waterlogged PBF fuel rod would propagate to the surrounding rods. A single power burst of 670 MJ was planned to produce a fuel enthalpy in the waterlogged test rod (the center rod in the nine cluster) 1.6 times greater than the failure threshold determined for PBF rods during previous CDC tests. The data obtained for this indicated that the test rod had not failed. A subsequent 670-MJ test resulted in failure of the test rod and generation of an 8-MPa pressure spike.

Posttest examination revealed that failure of the waterlogged rod damaged adjacent fuel rods in the test cluster, but did not result in fuel dispersal from the adjacent rods. Completion of this test without failure propagation provided assurance that the PBF core can be operated in a burst mode at energies beyond that at which waterlogged fuel failure would occur.

## 1.2 Reactivity Initiated Accident (RIA) Test Series

Z. R. Martinson, R. S. Semken, T. Inabe, and R. H. Smith

The Reactivity Initiated Accident Scoping Tests (RIA-ST) were introductory to the RIA Series 1 tests. The primary objectives of the scoping tests were defined as follows:

(1) Determine the applicability of extrapolating low-power, steady state calorimetric measurements and self-powered neutron detector (SPND) output to determine fuel rod energy depositions during a power burst

(2) Determine the energy deposition failure threshold for unirradiated fuel rods at boiling water reactor hot-startup coolant conditions

(3) Determine the magnitude of possible pressure pulses resulting from rod failure

(4) Determine the sensitivity of the test instrumentation to high transient radiation exposures.

1.2.1 Test Design. The RIA Scoping Tests comprised four, separate, single-rod experiments: Tests RIA-ST-1, RIA-ST-2, RIA-ST-3, and RIA-ST-4. The fuel rod for each test was positioned in a separate flow shroud in the center of the PBF in-pile tube. The first three tests were performed with 5.8-wt% enriched uranium dioxide fuel with 9.70-mm-diameter zircaloy-4 cladding. The fourth test was performed with

20-wt% enriched uranium dioxide fuel with 10.73-mm-diameter zircaloy-4 cladding.

Individual zircaloy-4 flow shrouds, having a nominal inner diameter of 16.3 mm and an outer diameter of 22.6 mm, surrounded the fuel rods of the first three tests. A zircaloy-4 flow shroud, having a nominal diameter of 19.3 mm and an outer diameter of 25.4 mm, surrounded the fuel rod of Test RIA-ST-4. Fuel particle catch screens were installed at the inlet and outlet of the flow shroud for Test RIA-ST-4, because at the high energy deposition rod failure was expected to produce free fuel particles.

Instrumentation was mounted on the test assembly for pressure pulse measurement, calorimetric measurement of the test rod power, and evaluation of instrumentation for future RIA tests. The test fuel rods were not instrumented. Figure 10 provides a schematic representation of the test train instrumentation.

1.2.2 Test Conduct. Nuclear test operation for the four tests included the following:

(1) Test RIA-ST-1: (a) power calibration period during which the test rod power with respect to PBF core power and to self-powered neutron detector (SPND) output current was determined, (b) a preconditioning period which caused cracking of the fuel pellets, and accumulation of a fission product inventory, and (c) two power bursts

(2) Test RIA-ST-2: nuclear operation was limited to a single power burst

(3) Test RIA-ST-3: nuclear operation was limited to a single power burst

(4) Test RIA-ST-4: (a) a power calibration period similar to that of RIA-ST-1, and (b) a single power burst.

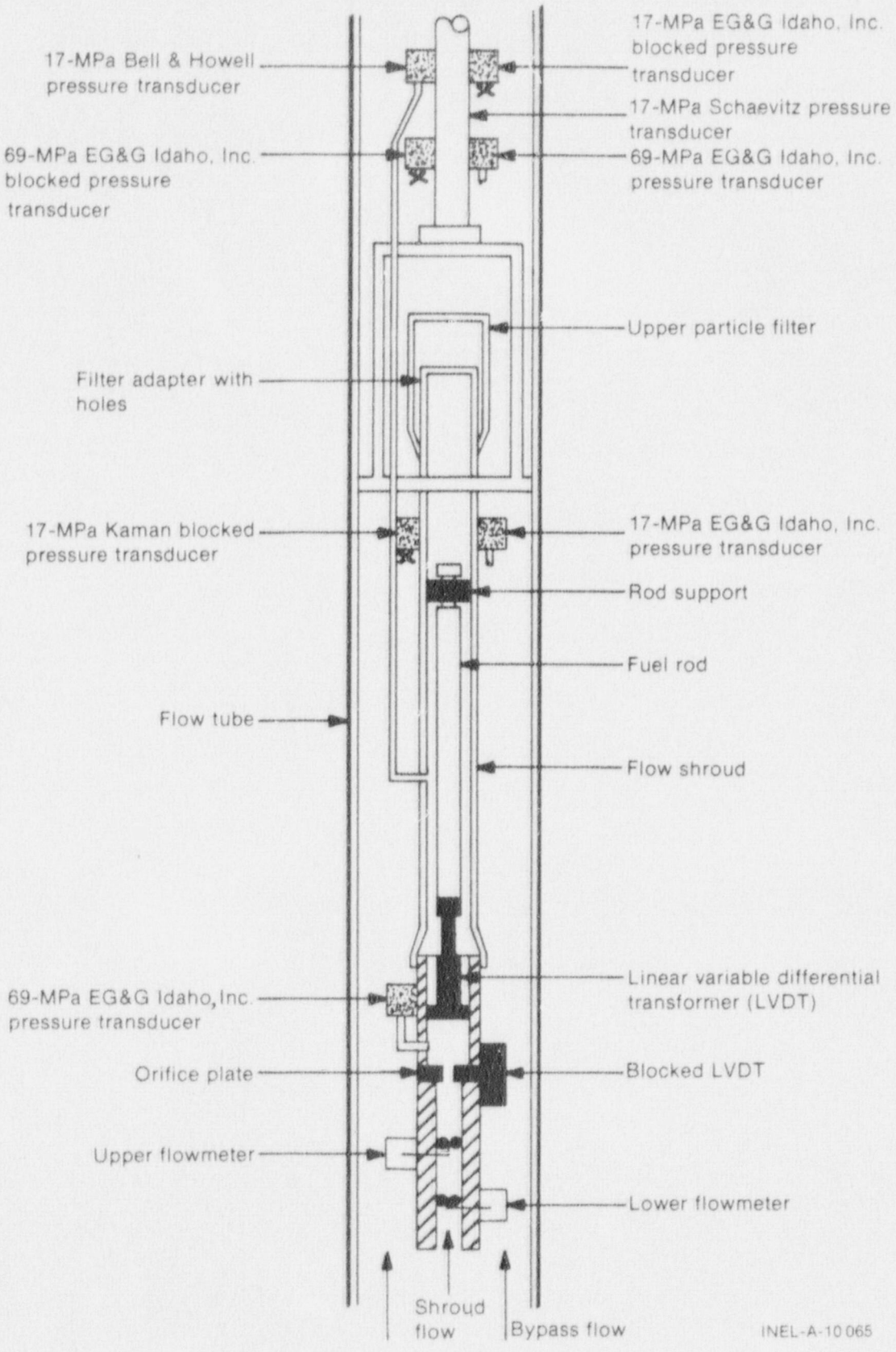


Fig. 10 Schematic cross section of test train for RIA Scoping Test showing approximate instrument locations.

1.2.3 Power Burst Conduct. The in-pile tube coolant conditions for each of the power bursts were approximately 85 $cm^3/s$ volumetric flow and 538 K temperature at the flow shroud inlet, and 6.45 MPa system pressure. Each power burst was initiated by rapidly increasing the reactivity of the reactor by the ejection of fast-moving control rods. Peak reactor power during the five power bursts ranged from 6500 to 16 000 MW.

The test rod energy deposition data for the four tests, which included five power bursts are summarized in Table I. Fuel rod failure occurred in all of the tests except Test RIA-ST-3.

TABLE I

RIA SCOPING TEST SUMMARY

| Test | Reactor Period (ms) | Total Radially Averaged Energy [a] (J/g $UO_2$) | Total Pellet Surface Energy [a] (J/g $UO_2$) | Rod Failure |
|---|---|---|---|---|
| RIA-ST-1 Power Burst 1 | 5.7 | 803 | 858 | No |
| RIA-ST-1 Power Burst 2 | 4.4 | 1020 | 1092 | Yes |
| RIA-ST-2 | 4.6 | 1000 | 1071 | Yes |
| RIA-ST-3 | 5.2 | 856 | 912 | No |
| RIA-ST-4 | 3.85 | 2205 | 3125 | Yes |

[a] Total energy includes 64 J/g $UO_2$ for ambient temperature of 538 K. Fuel rod energy values are based on the core ionization chamber data. Fuel rod energy values based on SPND output are about 25% higher.

(1) Test RIA-ST-1 Power Bursts. A total pellet surface energy of 858 J/g $UO_2$ at the axial flux peak was deposited during the first power burst. No indication of fuel rod failure was observed.

The second power burst of Test RIA-ST-1, performed on the same rod used in the first burst, deposited a total pellet surface energy of 1092 J/g $UO_2$ at the axial flux peak. Approximately 6 minutes after the power burst, rod failure was indicated by a plant radiation monitor located near the test loop piping. Rod failure was indicated about 1.5 minutes later by the fission product detection system. None of the pressure transducers or other test train instruments indicated the time of rod failure. The exact time of fuel rod failure is uncertain due to the long time necessary for coolant to flow from the fuel rod to the radiation monitor locations.

(2) Test RIA-ST-2 Power Burst. The Test RIA-ST-2 fuel rod was exposed to a single power burst with no significant steady state operation. The pellet surface energy at the axial flux peak was 1071 J/g. Neither the loop monitor nor the fission product detector indicated the fuel rod failure.

(3) Test RIA-ST-3 Power Burst. The Test RIA-ST-3 fuel rod was subjected to a single power burst which deposited a pellet surface energy of 912 J/g $UO_2$ at the axial flux peak. Neither the loop monitor nor the fission product detector indicated fuel rod failure.

(4) Test RIA-ST-4 Power Burst. After the power calibration was completed, the Test RIA-ST-4 fuel rod was subjected to a single power burst which deposited 2205 J/g $UO_2$ radially averaged at the axial flux peak or 3125 J/g

$UO_2$ at the fuel pellet surface. As expected, this large energy deposition resulted in immediate fuel rod failure. A 28.2-MPa pressure pulse was recorded by the lower 69-MPa EG&G pressure transducer connected to the lower end of the flow shroud. The time of the pressure increase was about 4 ms after the time of peak power. The fuel rod energy, radially averaged at the axial flux peak, was 1172 J/g $UO_2$ at the time of rod failure and corresponds to a fuel pellet surface energy of 1645 J/g $UO_2$.

The fission product detection system indicated rod failure about 3.25 minutes after the power burst. The loop radiation monitor indicated rod failure within 2 minutes after the power burst.

1.2.4 Test Results. Test results presented herein correspond to one of the four objectives of the RIA Scoping Test.

(1) Applicability of Calorimetric Measurements to Power Burst Testing. The first objective of the RIA Scoping Test was to evaluate the applicability of employing low-power calorimetric measurements to determine fuel rod energy depositions during a power burst. The use of radiochemical analysis to directly measure the power burst fuel rod energy deposition in the RIA Series 1 program tests will not be possible due to the use of preirradiated fuel and the extensive preconditioning operation of the fuel rods prior to the power burst. The irradiation of the fuel rods tested in Tests RIA-ST-2 and RIA-ST-3 was limited to single power bursts; therefore, radiochemical analyses will represent only the energy deposition during the power burst.

Two methods were used to determine fuel rod energy depositions. The calorimetric fuel rod power measurements

were related to the reactor ionization neutron detecting chambers located on the periphery of the core and also to the three SPNDs located on the test train. The energy deposition data obtained from the three SPNDs are about 25% higher than those obtained from the reactor ionization chambers. The reactor chamber values may be more accurate than the SPND-derived data because the core ionization chamber data were in excellent agreement with the pretest reactor physics calculations. In addition, if the SPND-derived fuel rod energy data are correct, then the fuel rod in Test RIA-ST-3 received a pellet surface energy of 1238 J/g $UO_2$ and did not fail. Fuel rod failure was predicted to occur at a pellet surface energy of 1096 J/g $UO_2$. The actual fuel rod energy depositions for the RIA Scoping Test power bursts will not be determined until the radiochemical analysis is completed.

(2) Failure Threshold. The second objective of the RIA Scoping Test was to determine the energy deposition failure threshold for the 5.8-wt% enriched fuel rods under commercial boiling water reactor hot-startup conditions. From the results of Tests RIA-ST-1, RIA-ST-2, and RIA-ST-3 (Table I), the failure threshold can be assumed to be between 912 J/g $UO_2$ where the fuel rod did not fail (Test RIA-ST-3) and 1071 J/g $UO_2$ where the rod did fail (Test RIA-ST-2), using the energy depositions determined from the output of the core ionization chambers. The pretest predictions indicated that the failure threshold would be 1096 J/g $UO_2$ at the pellet surface.

Figure 11 illustrates the posttest condition of the fuel rods from Tests RIA-ST-1, RIA-ST-2 and RIA-ST-3. The fuel rods from Tests RIA-ST-1 and RIA-ST-2 were fractured, whereas the Test RIA-ST-3 rod was intact. About

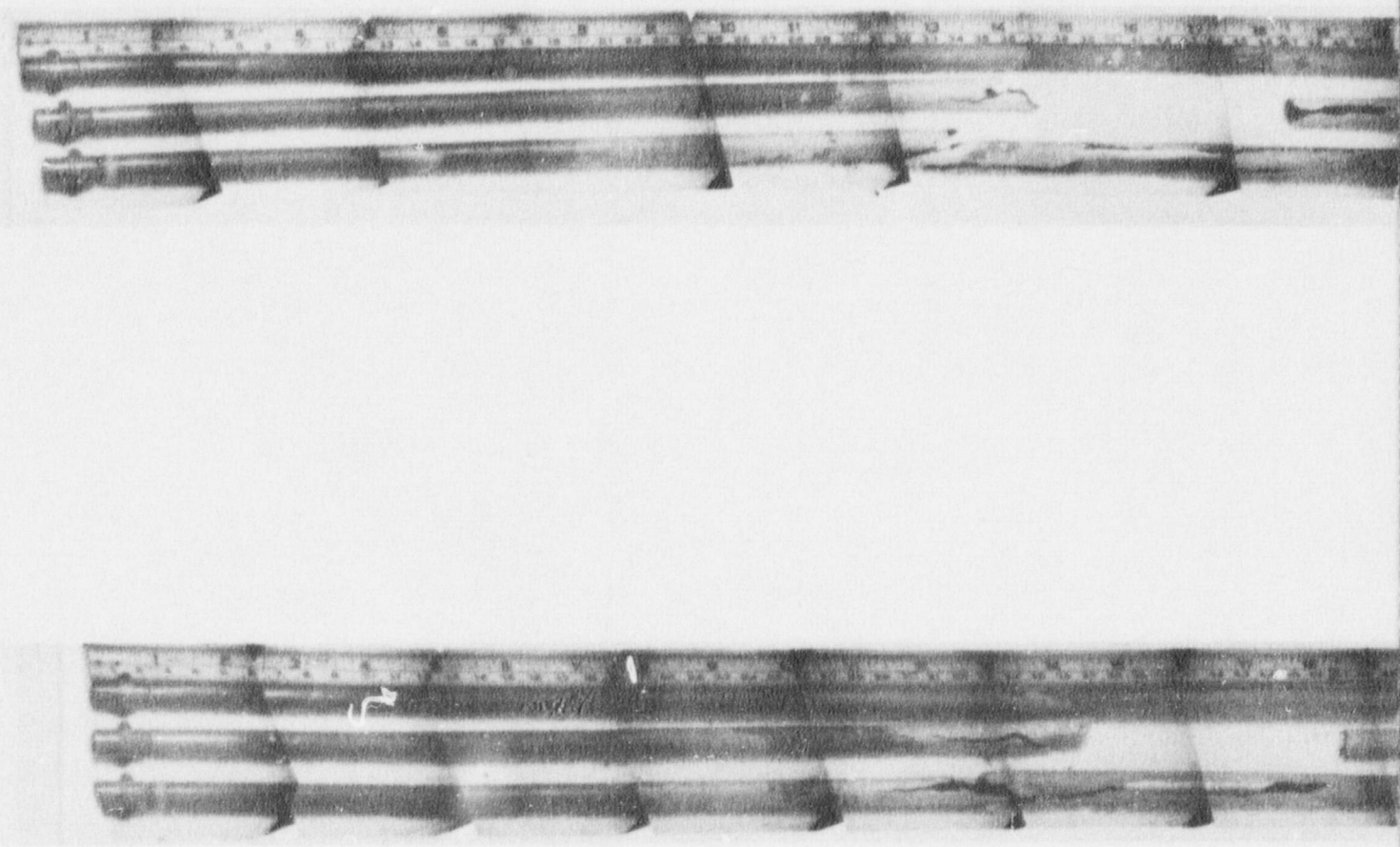

Fig. 11 Posttest condition of fuel rods and RIA-ST-3.

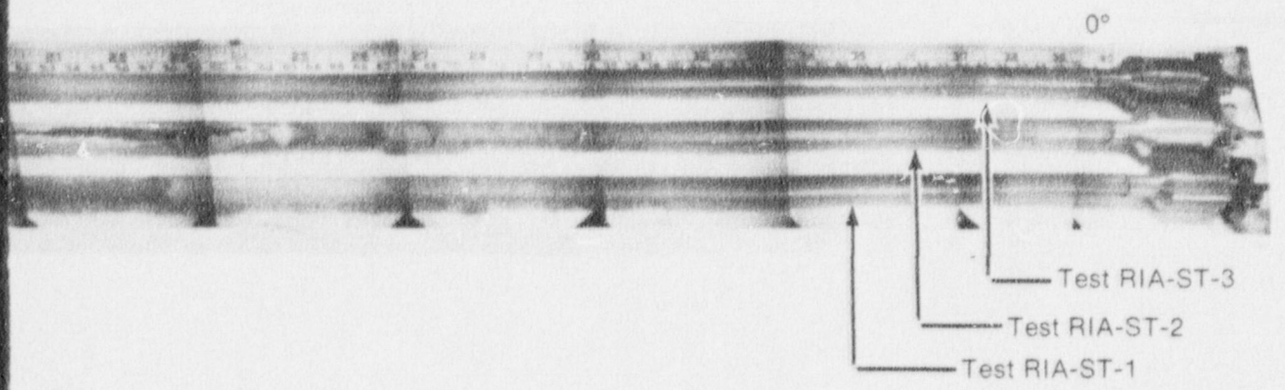


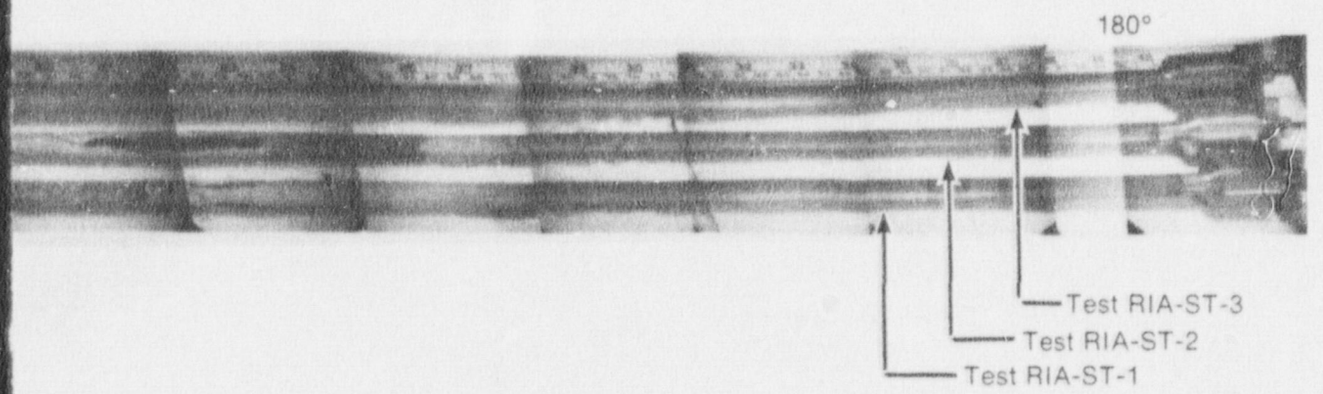


from Tests RIA-ST-1, RIA-ST-2,

59 g of fuel was gone from the Test RIA-ST-1 fuel rod and about 75 g from the Test RIA-ST-2 fuel rod. A longitudinal slit in the cladding of the Test RIA-ST-2 fuel rod was observed between the 0.52- and 0.60-m rod elevations in the zero- to 180-degree plane. The cladding in this region was extremely brittle and may have experienced melting. Bulging of the cladding at the pellet interface (bambooing) was observed between the 0.675- and 0.780-m rod elevations of the rod from Test RIA-ST-2. Small circumferentially oriented cracks occurred within the bulge.

Severe oxidation and cladding deformation of the Test RIA-ST-3 fuel rod were observed. No breaks in the cladding were detected. The cladding had collapsed into pellet interfaces and defects over most of the flux peak region. The Test RIA-ST-3 rod exhibited bambooing at only two pellet interfaces.

(3) Pressure Pulse Generation. The primary reason for the investigation into pressure pulse generation produced by RIA-induced rod failure is concern for the integrity of the PBF in-pile tube. No significant pressure pulses were measured for the first three tests. The Test RIA-ST-4 rod failure, however, was immediate and violent. Table II summarizes the pertinent data from each of the four pressure transducers used during Test RIA-ST-4.

The 17-MPa Bell & Howell pressure transducer, connected by a small-diameter tube to the inside of the flow shroud at the axial power peak location, saturated as a result of the large-source pressure pulse and did not provide the magnitude of the pressure pulse or a rise time. A 69-MPa EG&G pressure transducer fabricated by EG&G Idaho, Inc., was connected by a small-diameter tube

TABLE II

PRESSURE DATA FROM TEST RIA-ST-4 POWER BURST

| Pressure Transducer | Location | Pressure Increase (MPa) | Total Peak Pressure (MPa) | Rise[a] Time (s) |
|---|---|---|---|---|
| 17-MPa EG&G | Flow bypass near top of rod | 1.8 | 8.5 | 4 |
| 69-MPa EG&G | Upper plenum beyond particle screen | 2.1 | 8.9 | 3 |
| 69-MPa EG&G | Shroud inlet | 28.2 | 35.0 | 1.6 |
| 17-MPa B&H | Source region | 15.9 | 22.7 | [b] |

[a] Rise time is defined as the time from 10 to 90% of the pressure rise.

[b] Transducer saturated at a pressure increase of 15.9 MPa. Rise time time could not be obtained, but slope was approximately 20 MPa/ms.

into the inlet area of the flow shroud. The peak pressure rise was 28.2 MPa, with a rise time of 1.6 ms. The experiment predictions for the RIA scoping tests indicated that a 1987 J/g $UO_2$ energy deposition would result in a pressure pulse of 24.1 MPa, with pressure doubling of 31.7 MPa at 7 ms after fuel dispersal. The source pressure was attenuated outside the shroud region as indicated by the pressure transducers located in the upper plenum of the in-pile tube and in the flow bypass region. The 17-MPa EG&G pressure transducer, located outside the flow shroud near the top of the test rod, indicated a maximum pressure increase in the bypass region of 1.8 MPa with a rise time of 4 ms. The upper 69-MPa EG&G pressure transducer, located above the shroud outlet beyond the upper particle filter, indicated a pressure increase of 2.1 MPa with a rise time of 3 ms.

(4) Instrument Sensitivity. The final objective of the RIA Scoping Test was to determine the sensitivity of the test instrumentation to extremely high, short duration radiation exposures. This information is essential for proper data evaluation in the RIA Series 1 tests. To facilitate the instrumentation evaluation, several environmentally isolated devices were added to the test train.

In general, instrumentation sensitivity to radiation was minimal. The Kaman and Bell & Howell pressure transducers showed very little sensitivity to radiation. The EG&G pressure transducers indicated a slight sensitivity to radiation. A locked linear variable differential transformer (LVDT) also indicated only slight radiation sensitivity. The most significant instrumentation problem was a false full-scale flow rate indication by the flow turbines, apparently caused by the high radiation field during a power burst. The strain gages were also very sensitive to radiation.

## 2. PROGRAM DEVELOPMENT AND EVALUATION

W. J. Quapp and P. E. MacDonald

Activities associated with the PBF program development, coordination with foreign experimental programs, Nuclear Regulatory Commission (NRC) technical assistance, analysis of PBF test results, Halden fuel behavior research, and postirradiation examinations of commercial power reactor fuel are summarized.

### 2.1 Program Development and NRC Technical Assistance

D. W. Croucher

Preparation of requirements for an operational transient and anticipated transient without scram (ATWS) experiment was initiated. The fuel behavior predictions for BWR and PWR operational transients and

ATWS events were reviewed and categorized. Pellet-cladding interaction, cladding collapse, and cladding oxidation are potential fuel rod damage mechanisms during the transient. Simulation of a recirculation flow control failure with increasing flow in a BWR has been tentatively selected as an additional test to be conducted as part of Test GC 2-4 of the Gap Conductance Test Series.

## 2.2 PBF Test Analysis Results

D. W. Croucher, A. W. Cronenberg, S. L. Seiffert, M. S. El-Genk, and K. Vinjamuri

Accomplishments during this quarter included (a) completion of a report entitled "Light Water Reactor Fuel Response During Reactivity Initiated Accident Experiments"[13], and (b) an assessment of oxidation and embrittlement of zircaloy-4 cladding from high temperature film boiling operation. Assessment of fuel pellet fragmentation during a PCM event continued. Studies in the areas of molten fuel-cladding interaction and fission gas behavior during PCM events were initiated.

2.2.1 Light Water Reactor Fuel Response During Reactivity Initiated Accident Experiments[13]. Existing test results, data correlations, and interpretations relevant to the current understanding of light water reactor fuel behavior under conditions of a reactivity initiated accident are summarized in the referenced report. Experimental data are included from test programs previously carried out in the Capsule Driver Core (SPERT Project) and TREAT facilities at the Idaho National Engineering Laboratory and currently ongoing in the Japanese Nuclear Safety Research Reactor. Test results are summarized, primarily as derived from the literature, in terms of the thresholds, modes, and consequences of fuel rod failure. The effects of fuel rod design variations, environmental variations, elevated burnup, and fuel waterlogging are described. The data are correlated and analyzed to illustrate trends and salient features. Where possible, interpretations are made in terms of basic fuel properties and capsule environment.

2.2.2 Oxidation and Embrittlement of Zircaloy-4 Cladding From High Temperature Film Boiling Operation. The power-cooling-mismatch and irradiation effects test data on fuel rod cladding behavior were evaluated. Cladding embrittlement resulting from the high temperature oxidizing reactions with the coolant and the fuel was evaluated and compared with failure criteria. The in-pile data were correlated with room temperature embrittlement criteria based on the fraction of remaining beta-phase, the total extent of oxidation, and the mean oxygen concentration near saturation in the beta-phase. The applicability of other failure criteria was examined. The results show that the in-pile data are most consistent with criteria based on the mean oxygen content in the beta-phase, which indicates that time and temperature have a critical effect on the ultimate cladding oxygen distribution and on the extent of cladding embrittlement.

## 2.3 Halden Fuel Behavior Research

D. E. Owen, S. J. Dagbjartsson, A. D. Appelhans, M. E. Waterman

Analyses were completed of pellet-cladding interaction (PCI)[14] and thermal response[15] of fuel rods in Halden Assembly IFA-226, a mixed-oxide $(U\text{-}Pu)O_2$ assembly. The data obtained from the assembly and analyzed in both areas provided important information relevant to the understanding of the behavior of mixed-oxide fuel elements.

Data collection and analyses for the IFA-429 assembly were continued with emphasis on the evaluation of the power distributions within the assembly clusters which are governed by the silver shields surrounding the clusters during normal operation.

Pressure measurements and postirradiation examination on the IFA-429 fuel rods indicate that helium fill gas is absorbed into the $UO_2$ fuel in pressurized fuel rods. The IFA-429 fuel absorbed 0.0057 $cm^3$ (at standard temperature and pressure) of He/g $UO_2$. The absorption occurred during the first several months of operation and was larger in low density (91%) and small-grain-size fuel. The effective diffusion coefficient is $\sim 1 \times 10^{-8}$ $cm^2/s$. The [illegible]tude

of this coefficient, which is $\sim 10^5$ larger than the lattice diffusion coefficient, suggests that short circuit diffusion paths such as grain boundaries, irradiation-induced vacancies, or fission fragment injection are the dominant helium absorption mechanisms.

The NRC Halden Assembly IFA-430 will be placed in the reactor later this calendar year. In-depth preparation for the startup of the assembly was performed, which included analysis of gas flow tests conducted on dummy rods, and specifying of startup test operations. The startup operation is expected to provide a valuable data base for the evaluation of fuel cracking and relocation early in life.

## 2.4 Postirradiation Examination of Commercial Power Reactor Fuel

D. E. Owen

An apparatus was fabricated for the chemical decrudding of commercial fuel rods, a process that involves two chemical treatments at 360 K followed by a high pressure rinse.

An inert atmosphere cutting box was fabricated in which commercial fuel rod sectioning can be performed in a dry argon environment. Separate shipping canisters for inert atmosphere transportation were also fabricated. This technique of sectioning and shipping will preserve the fuel rod internal fission product chemistry while the samples are transferred to an inert atmosphere hot cell for detailed metallographic examination.

# IV. CODE DEVELOPMENT AND ANALYSIS PROGRAM

P. North, Manager

The Code Development and Analysis Program has the primary responsibility for the development of codes and analysis methods. The program provides the analytical research aimed at predicting the response of nuclear power reactors under normal, off-normal, and accident conditions. The codes produced in this program also provide a valuable analysis capability for experimental programs such as Semiscale, LOFT and the Thermal Fuels Behavior Program.

The development of the reference code, RELAP4, continued with the incorporation of the best estimate fuel model into the blowdown version of RELAP4/MOD7. Various other improvements, including a self-initialization capability, were also integrated into the code; and the blowdown version, RELAP4/MOD7 V2, was released to the NRC and other national laboratories.

In the area of the advanced codes, the application of the primary systems code, RELAP5, to the calculation of the Semiscale Mod-1 Isothermal Blowdown Test S-01-4A, was completed. The results of this calculation are presented in Section 1 below. The BEACON/MOD2A code development continued with the incorporation of a wall heat transfer calculation capability. Testing and checkout of this capability are currently in process.

In the area of fuel rod modeling, an uncertainty analysis procedure was incorporated into FRAP-T5 to allow the effects of various fuel rod input uncertainties on the calculated rod behavior to be determined. This procedure is discussed in Section 2. The development of MATPRO proceeded with the completion of work on fuel creep, hot pressing densification, and swelling.

## 1. RELAP5 APPLICATION TO SIMULATION OF SEMISCALE TEST S-01-4A

K. E. Carlson and H. H. Kuo

The RELAP5 code is an advanced, one-dimensional, fast-running system analysis code to provide an economic, best estimate (BE) and evaluation model (EM) transient analysis capability for use in calculating the transient behavior of light water reactors (LWRs). The technology and experience gained from the RELAP4 series of codes has led to this completely new code being developed, with a top-down structure and nonhomogeneous and nonequilibrium hydrodynamic modeling.

The RELAP5 code now includes models for most of the processes which occur during blowdown of a light water reactor and can be used to analyze interconnected components. Component models are included for pipes, branches, abrupt flow area changes, pumps, check valves, trips, heat exchangers, and break flows. These models are integrated into a general purpose and user convenient system code framework. The code is operational and has been tested on several separate effects two-phase flow experiments and hypothetical test problems. Generally, good agreement with experimental data and fast computer run times have been achieved.

A recent application of the RELAP5 code has been the modeling of a Semiscale isothermal blowdown experiment (Test S-01-4A). Semiscale Test S-01-4A is a counterpart to the LOFT Test L1-4. The Semiscale Mod-1 Test S-01-4A was conducted with a 200% cold leg break and with ECC injection into the cold leg of the intact loop. The initial isothermal temperature was 555 K and the initial system pressure was 15.6 MPa. The blowdown experiment was modeled up to 60 seconds, approximately the time of ECC accumulator emptying. This period includes ECC injection from 22 seconds to 60 seconds. Generally, the calculated results are in agreement with the data.

The calculations early in time in the blowdown experiment show some thermal nonequilibrium effects whereas the long-term results demonstrate significant nonhomogeneous flow effects. Examples of such

phenomena are ECC mixing, ECC bypassing, and countercurrent flow in the downcomer.

The calculational time for the RELAP5 simulation of the Semiscale isothermal blowdown to 60 seconds was 54 minutes of CDC 7600 CPU time.

## 1.1 RELAP5 Semiscale Mod-1 System Model

RELAP5 input is component oriented and each component can be subdivided into a system of subcontrol volumes. None of these components are modeled as active heat sources. Only the stored energy due to the initial system temperature is considered. As depressurization and flashing occur, however, significant wall-to-fluid temperature differences are developed. As a result, wall heat transfer is an important phenomenon.

The use of RELAP5 to simulate the Semiscale Mod-1 system is the first full-system application of RELAP5. Although results in good agreement with data were obtained the results do not represent a comprehensive modeling study. The code results are presented in order to demonstrate the current RELAP5 capability.

## 1.2 Calculated Results

The long-term calculations were carried out to 60 seconds (approximately the time of accumulator emptying and nitrogen injection into the system). Injection of 302 K ECC water was begun at 22 seconds and was continued throughout the remainder of the simulated transient (60 seconds).

The pressure response in the first 0.5 seconds is shown at the vessel side of the break in Figure 12. The calculated pressures are in qualitative agreement with the data. Only the higher frequency character of the data is not reproduced.

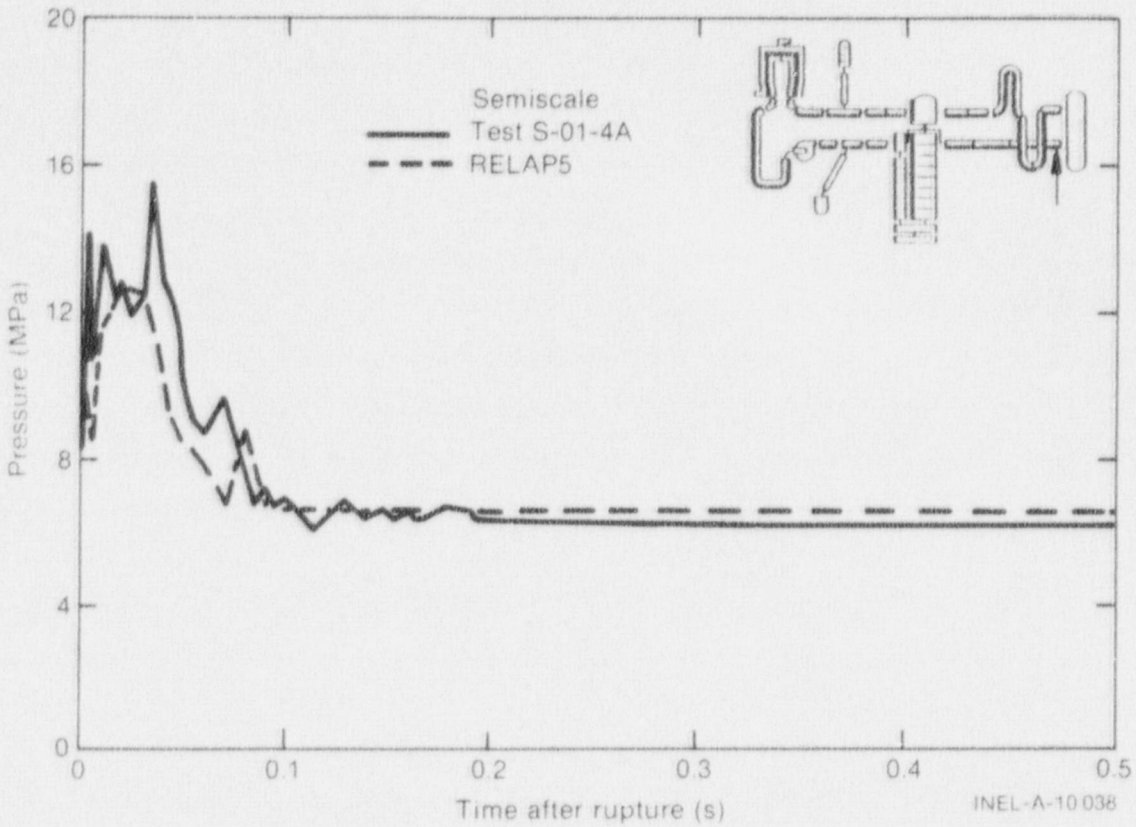


Fig. 12 Comparison of RELAP5 calculations with measured data from Semiscale Test S-01-4A for short-term pressure response at vessel side of break.

The system pressure and the pressurizer pressure are shown in Figure 13. The pressure is in good agreement up to 20 seconds and the point of liquid emptying, the break in the curve at approximately 10 seconds, is in good agreement with the data. The calculated pressures beyond 20 seconds are higher than the data due to the assumption of excessive heat transfer. Results without heat transfer are in better agreement with the data. The calculated system pressures at the break are in good agreement with the data up to 20 seconds and are too high thereafter, again due to the assupmtion of excessive heat transfer.

The calculated densities are compared with the data in Figure 14. Most of the calculated densities show an early drop compared with the data. This difference can probably be explained by the fact that the actual vapor formation is mostly at the walls which would lead to an inverted annular flow with low interphase drag, while the calculational

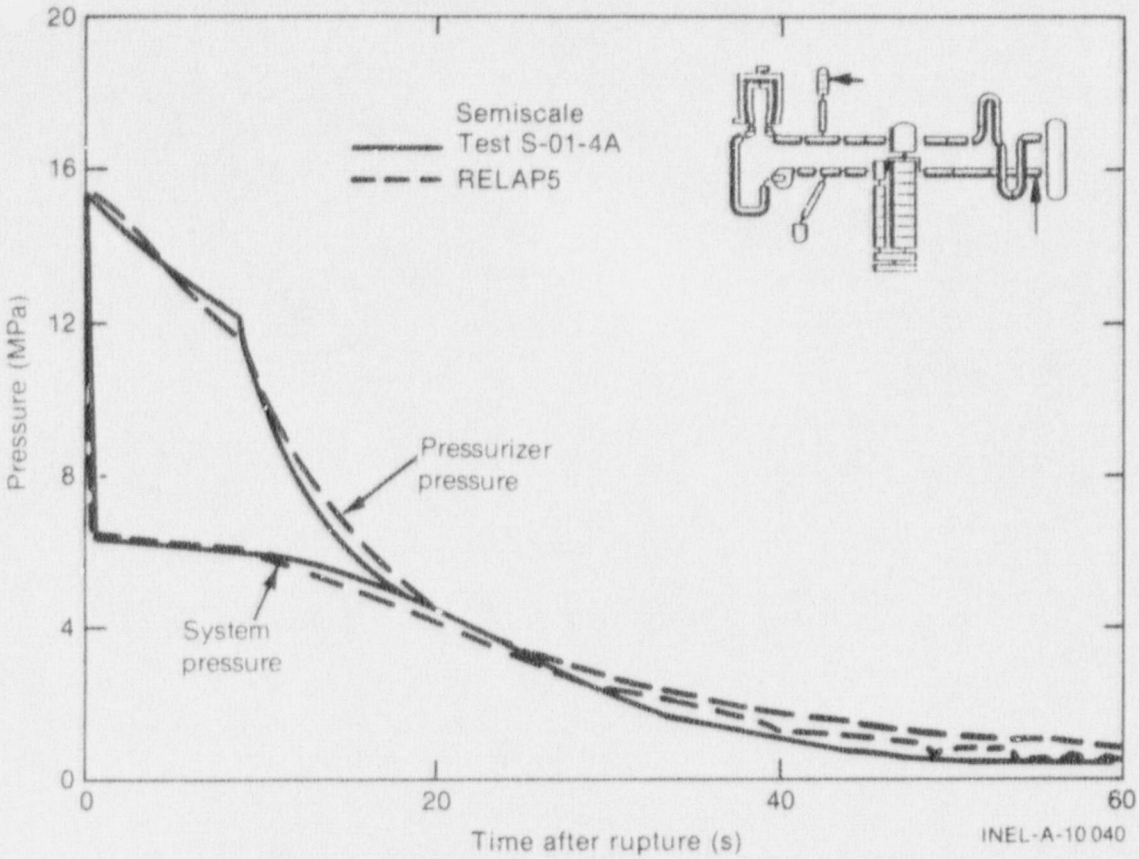


Fig. 13 Comparison of RELAP5 calculations with measured data from Semiscale Test S-01-4A for system pressure and pressurizer pressure.

model assumes a bubbly dispersed flow with high interphase drag. Because the calculated slip is less, greater liquid transport results. After ECC injection begins, the calculated results are markedly similar to the data as slugs of liquid are transported through the system.

The calculated break mass flow is compared with data in Figure 15. Here again good agreement with data is obtained. The early time flow at the vessel side of the break is high, for about 8 seconds, and is consistent with the early drop in density calculated to exist at most points in the system. Vapor formation at the walls and inverted annular flow would result in a lower mass flow at the break. Slugs of ECC water arriving at the break cause peaks in mass flow rate which occur at approximately 50 seconds.

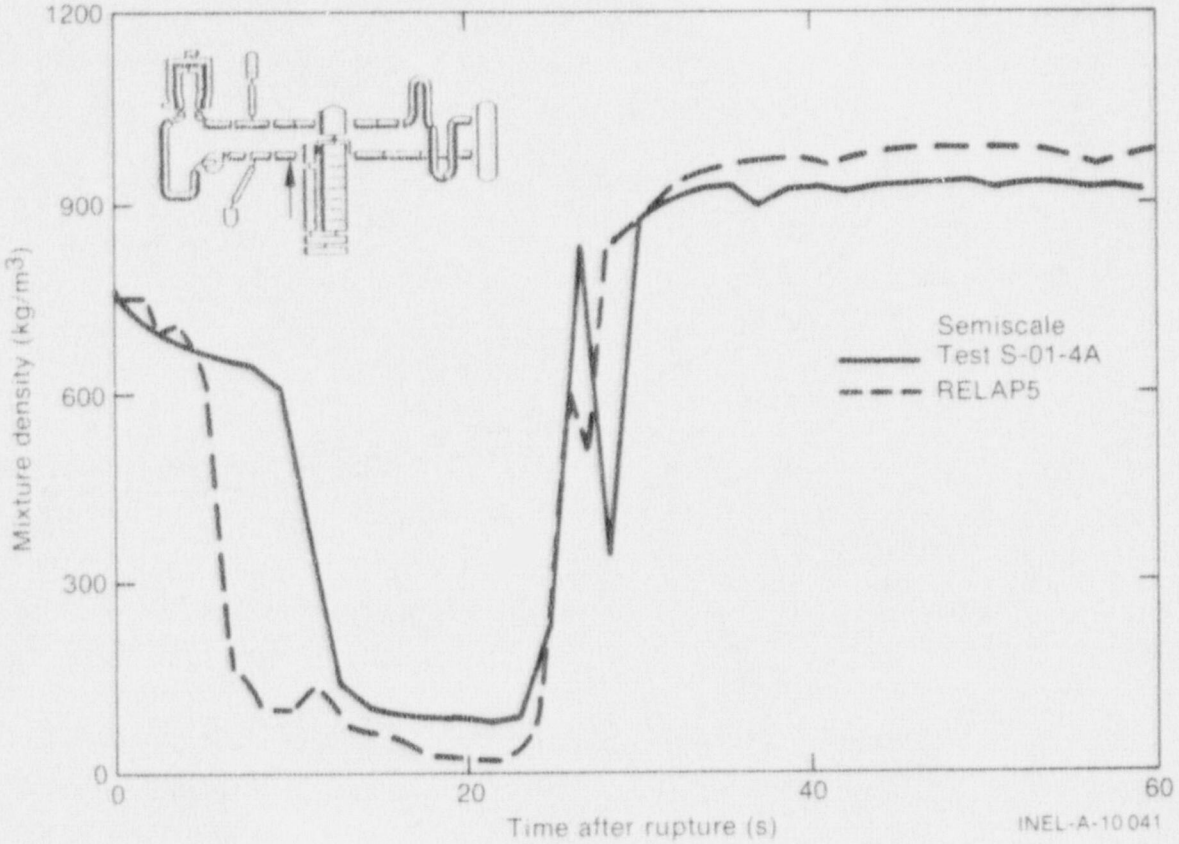


Fig. 14 Comparison of density calculated by RELAP5 with measured data from Semiscale Test S-01-4A.

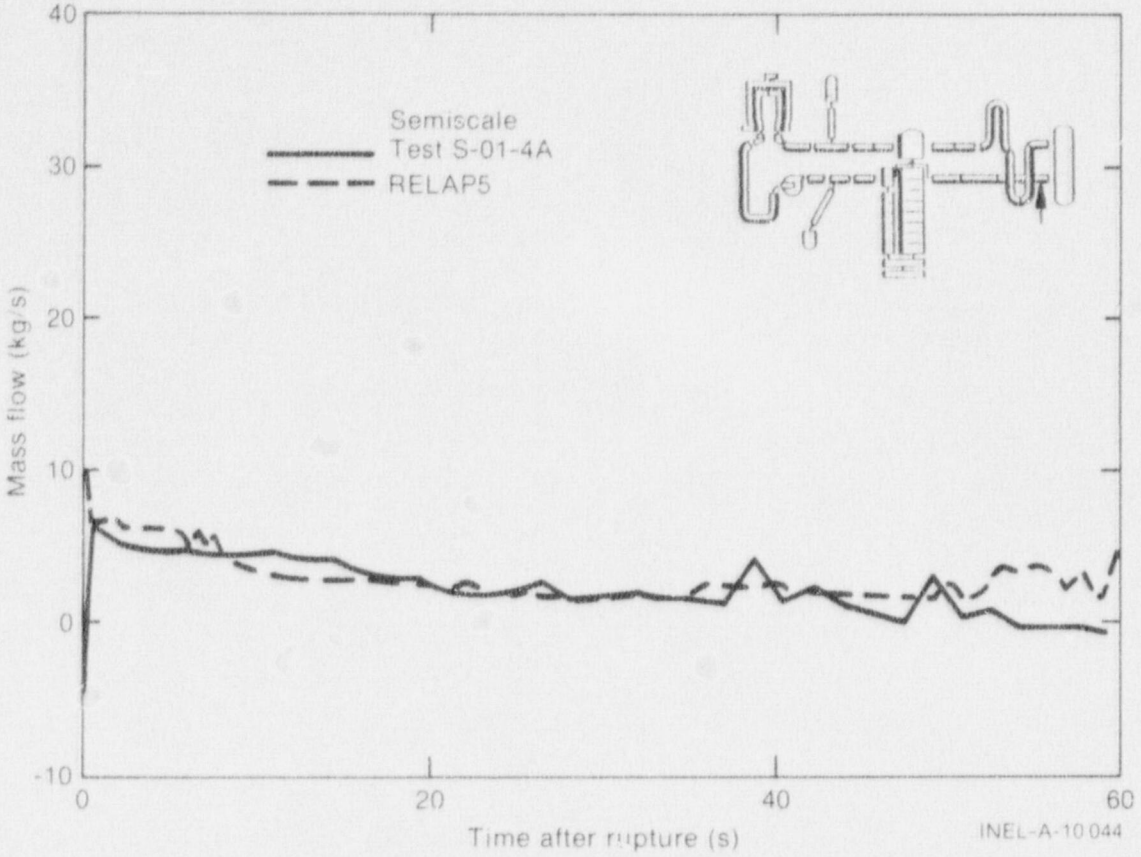


Fig. 15 Comparison of break mass flow rate calculated by RELAP5 with measured data from Semiscale Test S-01-4A.

## 2. UNCERTAINTY ANALYSIS OF THE FRAP CODE

Scott O. Peck

A user-oriented, automated uncertainty analysis capability has been incorporated in the Fuel Rod Analysis Program (FRAP) code and has been applied to the calculation of a pressurized water reactor fuel rod undergoing a loss-of-coolant accident. In calculations the fuel rod geometry and material properties were varied statistically, but the fuel rod initial conditions and the thermal-hydraulic boundary conditions were held fixed. The automated uncertainty analysis version significantly reduces the time required to complete the code uncertainty analysis and, at the same time, greatly increases the problem scope (the number of statistically varying inputs). Results of the fuel rod uncertainty analysis have shown a significant difference in the total and relative contributions to the uncertainty of the response parameters between steady state and transient conditions.

## 2.1 Method of Analysis

The uncertainty analysis method selected for use with the FRAP code is the response surface method. In this application, a response is any output variable of a computer code calculation. Some functional relationship exists between a response and the input variables. For input variables, this relationship defines a surface, resulting in the term "response surface". When the code is rather simple, this surface may be determined analytically over the entire range of the input values. More often, as in the case of the FRAP code, the surface may be known only through the code, and the range of inputs and problem types is very large. Consequently, the complete, true response surface cannot be determined analytically. The response surface method of uncertainty analysis is based on a systematic sampling of the true surface, which is then approximated by a polynomial equation for the independent (input) variables. In effect, a smooth surface approximates the true surface[16].

Without excessive cost, the polynomial approximation to the true response surface may be used to examine the behavior of the true surface in the region of the sample space. In particular, the polynomial can be used to study the propagation of errors through the code and the effect of the errors on the uncertainty in computed outputs. Thus, the response surface method may be used to obtain an estimate of response uncertainty and the relative contributions of input variables to this uncertainty.

## 2.2 Implementation

The primary objective of this work was not only to assemble an uncertainty analysis method, but also to incorporate it in the FRAP code as an automatic user option. With this option, the user is required only to define a nominal base case, choose the degree of the polynomial approximation, and select code responses and input variables. The code includes default uncertainty factors for over 50 input

variables; these factors may be easily updated. After the code automatically establishes an experimental design, the code will then perturb the independent variables of the nominal case according to the experimental design and compute the required cases of the problem. Finally, the code estimates the response equation coefficients and uses second-order error propagation techniques to determine the response uncertainties. Thus, the user has a complete uncertainty analysis in a single computer run. This capability represents a significant departure from the usual necessary practice of making a large number of individual analyses. As a result, the time required to complete an uncertainty analysis of the FRAP code will be reduced from months to a few days.

## 2.3 Application

Calculations illustrating the use of the FRAP uncertainty analysis method have been completed. The base case was a nominal PWR fuel rod subjected to a 200% cold leg break LOCA at 100% power. Thirty-seven input variables representing almost all material properties and fabrication parameters, and a few operating conditions, were chosen as independent variables. Seven responses selected from both thermal and mechanical parameters were used as dependent variables. Since the fuel rod response during a transient can be significantly affected by variations in thermal-hydraulic boundary conditions, the results of the calculations are conditional. A more realistic analysis would have to include nondeterministic boundary conditions. However, when these conditions are available (either from analysis or experiment), they can easily be incorporated in the uncertainty analysis structure as currently programmed.

Figure 16 shows the nominal calculated rod cladding surface temperature with a calculated uncertainty of one standard deviation due to fuel rod related uncertainties. Figure 17 shows the fractional contributions to the total variance of cladding surface temperature of the seven most influential fuel rod variables in the analysis. As the calculation of the problem progresses, both the absolute and relative

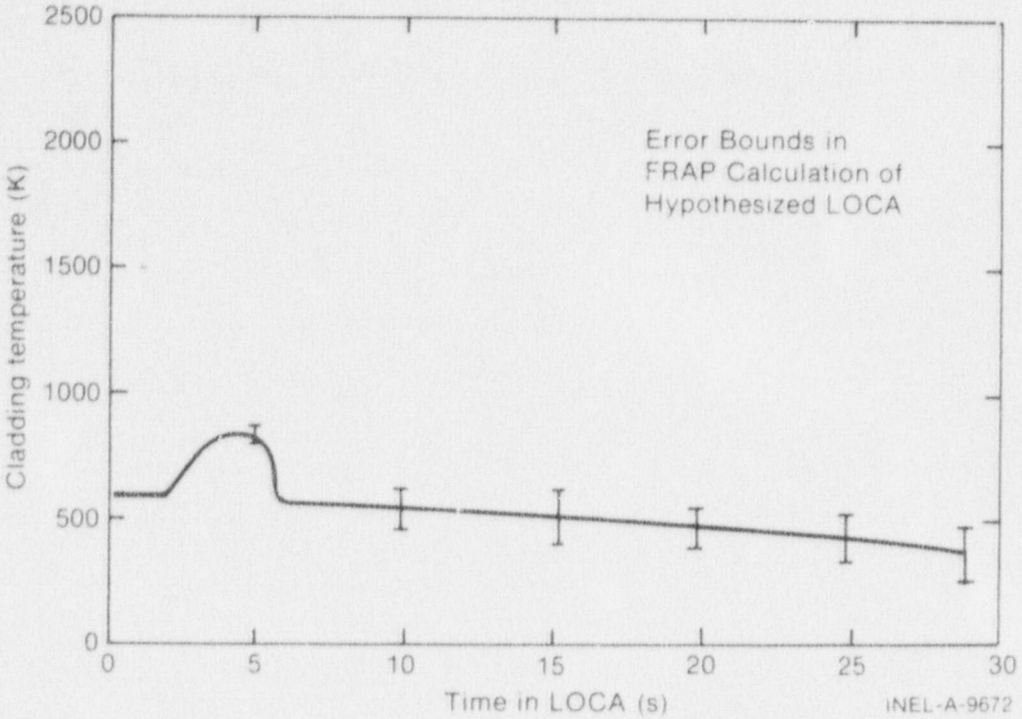


Fig. 16 Calculated rod cladding surface temperature during a LOCA and calculated uncertainty of one standard deviation from nominal resulting from uncertainties associated only with fuel rod input parameters.

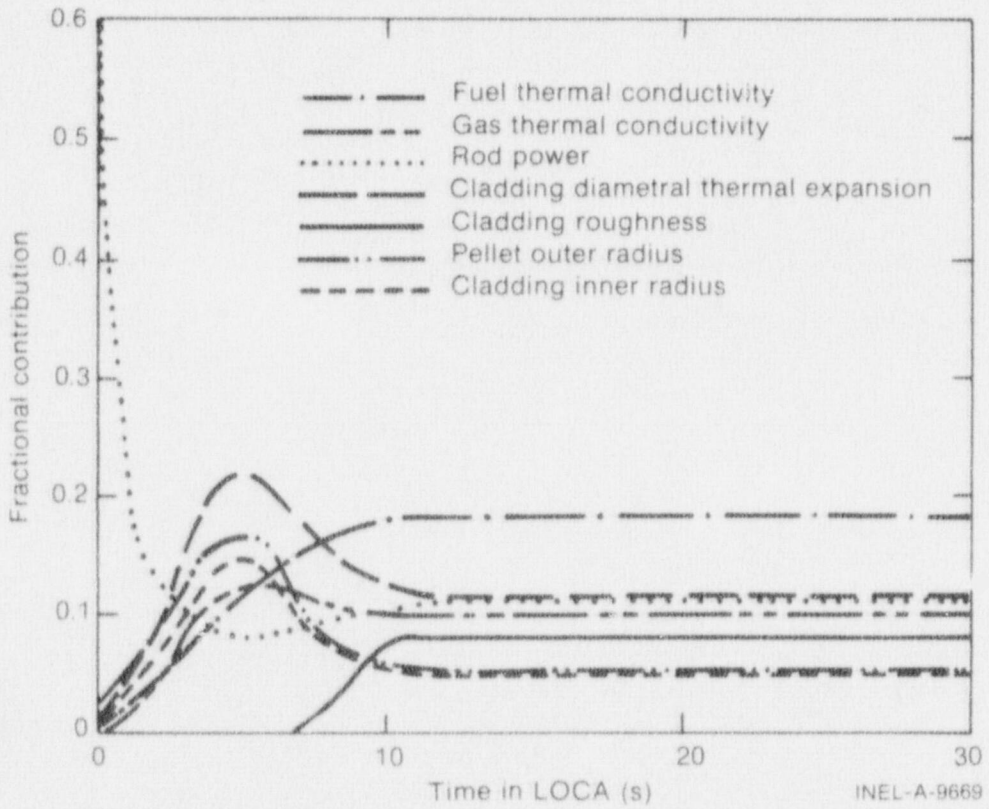


Fig. 17 Fractional contribution to variation of rod cladding surface temperature of seven most influential fuel rod variables.

contributions of different variables to the total uncertainty are shown to vary significantly.

These results demonstrate how an uncertainty analysis can be used to identify the significant sources of uncertainty in a computed response. Such knowledge provides insight with which to formulate direction for planning experimental programs and code development efforts.

# V. CODE ASSESSMENT AND APPLICATIONS PROGRAM

J. A. Dearien

The Code Assessment and Applications Program performs independent computer code assessment, technical surveillance of NRC/Industry cooperative programs, and the development and maintenance of the NRC/RSR data bank.

Computer codes undergoing independent assessment are the RELAP4/MOD6 thermal-hydraulic code and the fuel rod codes FRAP-T and FRAPCON. The major portion of the RELAP4/MOD6 assessment was completed this quarter. Assessment of FRAP-T4 was completed, and preparation for the assessment of FRAPCON-1 was initiated.

In the technical surveillance area, participation in NRC-Industry programs was continued. The jet pump testing program was completed.

The NRC/RSR data bank development was continued with additional entries of test data to the bank.

## 1. LOCA ANALYSIS ASSESSMENT

T. R. Charlton, W. S. Haigh, and T. D. Knight

For RELAP4/MOD6 assessment, several comparisons were made of RELAP4/MOD6 calculations with pressurizer component data, system blowdown data for six Semiscale Mod-1 tests, Semiscale Mod-3 gravity reflood data, LOFT LOCE L1-5 data, and FLECHT, FLECHT-SET, and Semiscale Mod-1 reflood data.

The comparison of RELAP4/MOD6 calculations[a] with data from six Semiscale Mod-1 blowdowns indicated that the code provides a reasonable calculation of rod peak cladding temperature during the blowdown transient. Calculated heater rod temperature responses compare

[a] RELAP4/MOD6, EG&G Idaho, Inc., Configuration Control Number C00100005.

favorably with the data in the lower half of the core where critical heat flux (CHF) generally occurs early in the tests (between 0.5 and 1.0 s after rupture). For example, the calculated peak cladding temperature at the maximum power zone is within 60 K of the maximum measured temperature, as shown in Figure 18, which is about one standard deviation of the experimental data scatter at that power step. However, in the upper half of the core, the heater rod temperature response is calculated to be high by as much as 150 K, although the standard deviation in the experimental data scatter is about 20 K. The calculation of high temperature is due to delayed CHF (beyond 2.0 s into blowdown) in the experiment, whereas RELAP4/MOD6 calculates early CHF. In comparison with Semiscale data from tests with high radial power peaking (Test Series 6), the calculated temperatures in general were higher than the data by larger margins.

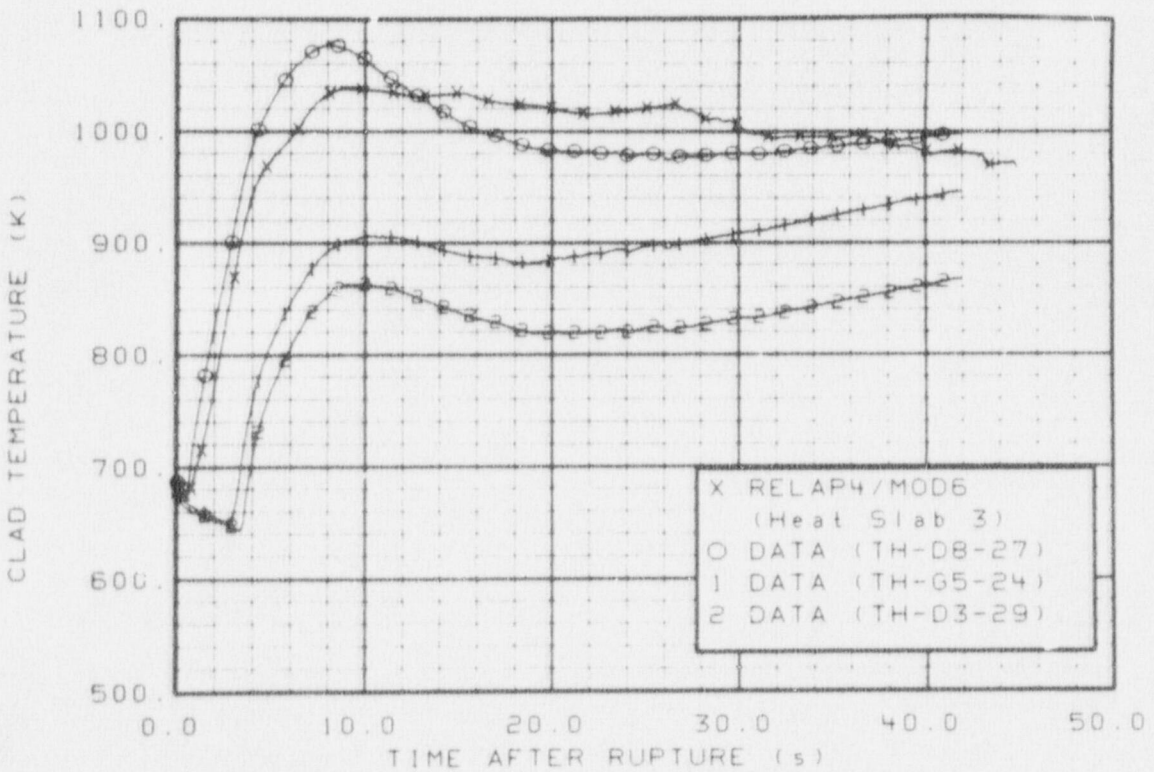


Fig. 18 Comparison of calculated and measured rod cladding temperatures for the high power step in Semiscale Test S-04-6 at 61-cm (TH-G5-24), 69-cm (TH-D8-27), and 74-cm (TH-D3-29) elevations above bottom of core heated length.

Calculated system pressures are lower than the data by about 500 kPa at 5 s to more than 1000 kPa near the end of blowdown. The lower calculated pressure has a corresponding effect on the calculated time to refill the system, which occurs at least 12 s early. Sensitivity studies were conducted to determine the effect of critical flow multipliers on the depressurization rate. During the subcooled blowdown period, the system pressure response is insensitive to the break flow multiplier, although the break flow is directly proportional to the multiplier. During the saturated blowdown period, the calculation of system pressure is very sensitive to the break flow multiplier as shown in Figure 19, with the break flow being insensitive to the multiplier.

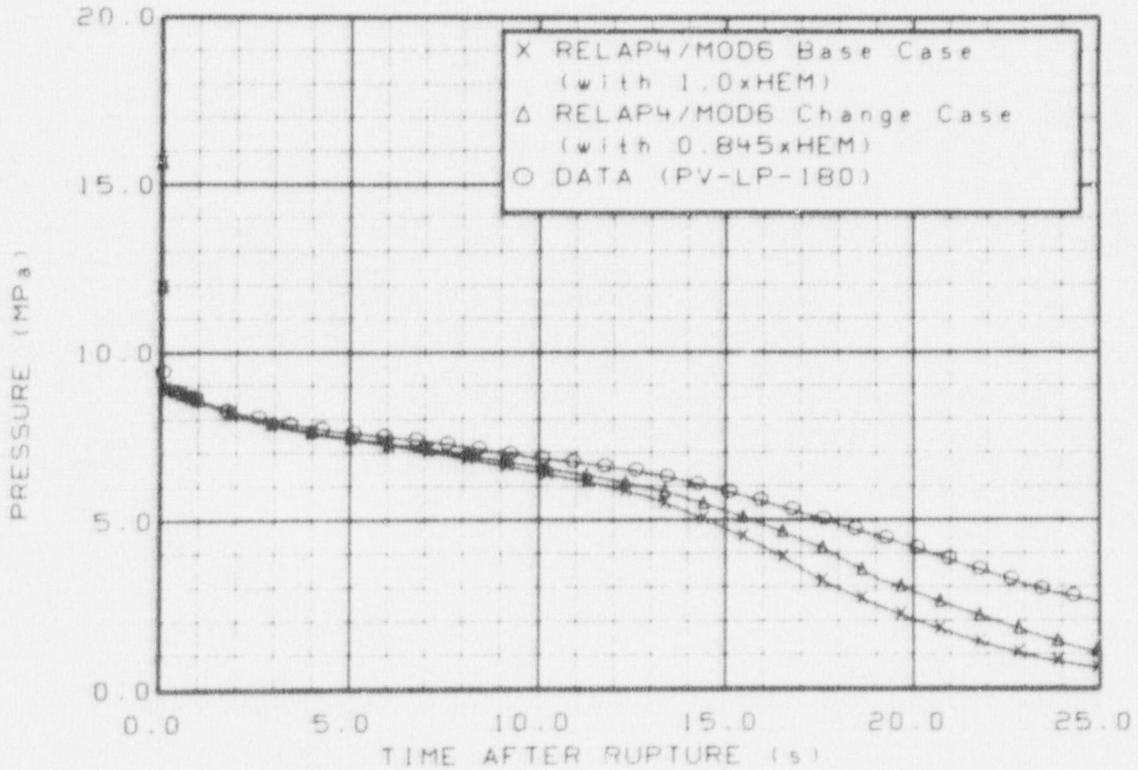


Fig. 19 Comparison of calculated and measured (PV-LP-180) system pressure for Semiscale Test S-06-1 showing calculated pressure sensitivity to multiplier on saturated critical flow model.

Improved guidelines for the selection of reflood heat transfer input options were developed using code-data comparisons of previously

analyzed gravity and forced-feed experiments. To check the applicability of the guideline revisions, additional FLECHT, FLECHT-SET, and Semiscale experiments were modeled using both the initial and revised guidelines. A calculation of FLECHT Skewed-Bundle Test 13404 (shown in Figure 20) demonstrates the improvement obtained with the new guidelines. Although the improvement at all core elevations and for all experiments was not as significant as that shown, a general improvement in agreement of calculations with data for cladding temperatures was obtained.

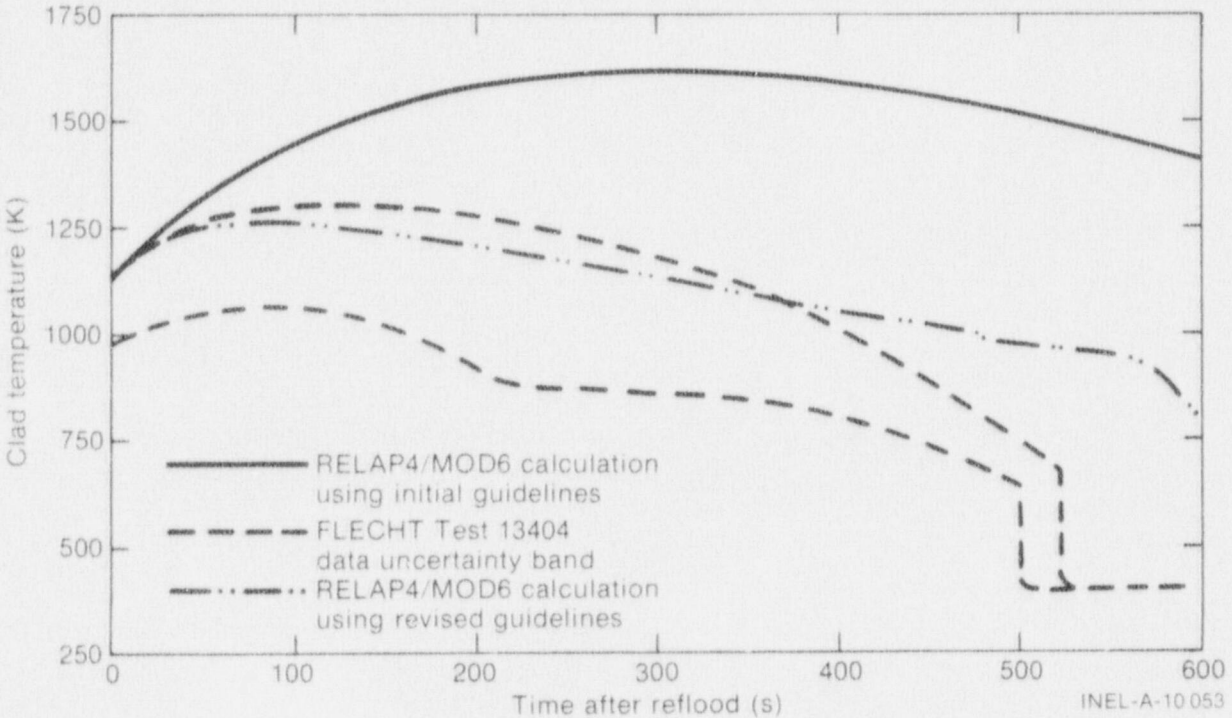


Fig. 20 Comparison of calculated and measured rod cladding temperature for FLECHT Test 13404 near core hot spot at 3.05-m elevation.

## 2. FUEL ANALYSIS ASSESSMENT

D. R. Coleman

FRAP-T4 capabilities for calculating pellet-cladding interaction (PCI) failures were assessed[17].

Calculated results from the transient Fuel Rod Analysis Program (FRAP-T4)[a] were systematically compared with measurements for rods

[a] FRAP-T4, Version 4, EG&G Idaho, Inc., Configuration Control Number H00340IB.

operating under off-normal and transient conditions. Critical heat flux, power ramp failures, and transient center temperature response were the fuel behavior areas addressed by comparisons to data for operating fuel rods. A series of out-of-pile tube rupture data comparisons was also performed. Best-estimate data comparison studies were preceded by standard rod scoping runs which established consistency between steady state FRAP-S3 results and initial FRAP-T4 conditions. Overall results indicate that more realistic treatments of pellet relocation effects on thermal and mechanical response are needed before integral accident analysis capabilities can be demonstrated.

The relocation adjustment to thermal conductivity in FRAP-T4 is stronger than that used in FRAP-T3. The relocation effect on internal void volume in FRAP-T4 is physically reasonable, but the assumed crack temperature causes an overprediction of internal pressure levels. The pellet repack factor is inconsistent with the relocation model data base. The coupling between relocation and the structural gap and effective conductivity calculations does not properly account for soft PCI pellet mechanical properties or crack closure.

The relative capabilities of the B&W-2, W-3, LOFT, and CE-1 correlations for calculating CHF flow and power conditions were evaluated using 78 PBF data points. The accuracy of the model in all cases was better for calculating CHF channel power under measured flow conditions than for predicting CHF flow at measured power levels. The models are all likely to calculate higher CHF power and lower CHF flow. The LOFT correlation best represents CHF conditions in PBF, followed by the W-3, B&W-2, and CE-1 correlations.

Comparisons between the measured and calculated influence of key fuel design and operating parameters on ramp induced cladding failure probability were used to evaluate the adequacy of PCI models. The comparisons indicate a need to incorporate or revise models for certain physical effects which are likely to accompany fuel temperature increases. The effects to be considered include relocation, crack

closure, fuel rate dependent and cladding deformation, prior irradiation effects on mechanical properties, disposition and diffusion of fission products, and gas retention.

Comparisons between measured and calculated transient fuel thermal response during 32 reactor shutdowns were made based on center initial temperature, thermal decay constant, and equilibrium temperature. An upper limit should be imposed on how much relocation can occur for rods with relatively large gaps (>2%). Decay constants were generally calculated to be lower, but were always within 25% of the data. Overpredicting fuel temperatures and underpredicting transient relocation resulted in limited crack space availability and led to an overestimation of effective pellet conductivity. Pellet conductivity effects on model accuracy could not be distinguished due to equivalence of the effects of cladding, gap, and fuel temperature differences at low power initial stored energy.

Comparison of FRAP-T4 results with data from two TREAT LOCA simulation tests showed that surface temperature response under single phase steam cooling conditions was well represented by the model[18,19]. The larger plenum rod pressure response was adequately calculated, but relocation effects resulted in overprediction of the pressure response in the large gap, small plenum rod. Incorporation of strain rate dependence in the burst model improved predictions for time and duration of cladding rupture.

Comparisons between measured and calculated clauding rupture conditions were based on data from out-of-pile heated zircaloy tube tests. A special code version which bypassed all but the material property and mechanical response models was used. Burst temperature and pressure calculations are more accurate for alpha-phase material tested at high pressure and below 1100 K. Either cladding strength or instability strain is overestimated at higher temperatures. Failure strains are generally overpredicted.

## 3. TECHNICAL SURVEILLANCE OF NRC/INDUSTRY COOPERATIVE PROGRAMS

T. R. Charlton, E. E. Ross, and W. S. Haigh

The role of the Code Assessment and Application Program as technical advisor to NRC is to ensure that the data from the industry cooperative safety experimental programs are adequate for the assessment of LOCA analysis codes. The industry cooperative experiments are the BWR-BD/ECC (boiling water reactor-blowdown/emergency core cooling) program and the FLECHT-SEASET (full length emergency cooling heat transfer-separate effects and systems effects tests) program. In support of the BWR-BD/ECC Program, a jet pump testing program is being conducted.

### 3.1 Jet Pump Testing Program

Steady state single-phase tests were conducted on a 1/6 scale jet pump to obtain data for improving the jet pump calculational model. Two additional transient two phase tests were conducted to provide data for assessing model improvements.

Steady state tests were conducted at subcooled fluid conditions to determine jet pump behavior over a wide range of on and off-design flow rates and patterns. System pressure was varied from ambient to BWR operating conditions. Measurements of overall and internal jet pump behavior were taken at over two hundred points. One transient test had scaled flow rates and flow directions similar to those found early in a BWR LOCA. For the second transient test, flow was similar to a BWR broken loop with the drive flow reversed and choked at the nozzle.

An M-N curve, Figure 21, shows the overall jet pump behavior as developed from the steady state data. M is the ratio of suction to drive flow and N is the ratio of discharge minus suction heads to drive minus discharge heads. The curves are for a constant drive flow of 3 kg/s (forward and reverse). Results show that the M-N curves are essentially independent of drive flow rate. M-N curves also appear independent of temperature and pressure. Transient test results show

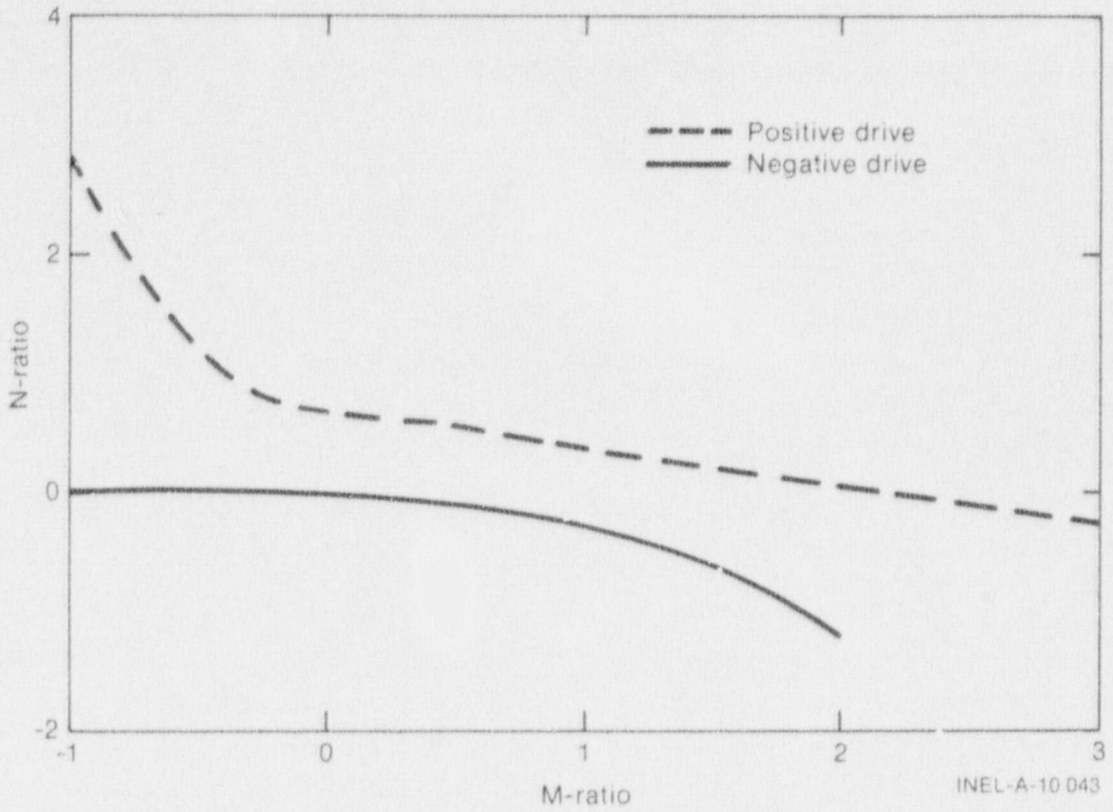


Fig. 21 Jet pump M-N curve.

that flow rates, direction, and quality in the jet pump were as specified.

## 3.2 BWR BD/ECC Program

Calculations were performed to examine the impact of an alternate reflood path on the TLTA system response. Modifications have been proposed to the TLTA-4 (Two Loop Test Apparatus, scaled to a BWR-6) facility to include (a) a pipe and control valve connecting the upper and lower plenums, (b) high pressure core spray, low pressure core spray, and low pressure core injection, and (c) the raising of the jet pump suction to 2.54 m above the bottom of the heated bundle. The valve in the alternate reflood path opens at 50 s into the blowdown transient.

Results of the calculations that were performed with RELAP4/MOD6 to examine the effect of the alternate reflood path on the transient indicate that temporary increases in lower plenum inventory resulted

from opening the valve. However, overall results showed little difference because of steam binding in the alternate reflood path.

### 3.3 FLECHT-SEASET Program

Test predictions were made for a steam generator reference (baseline) test that indicate that secondary fluid cooldown is a slow, stable process and that energy transfer from the secondary fluid is sufficient to vaporize all of the liquid introduced into the primary system throughout the 400 seconds analyzed. Extrapolation of the analysis results indicate that liquid will not pass through the steam generator within 1000 seconds. Peak heater rod surface temperature was calculated to be 1324.8 K and occurs just above midplane 96 seconds after reflood start. This same location is quenched 415 seconds after test initiation. Other heater rod quench times ranged from 8 seconds at the bottom of the core to slightly more than 600 seconds at 2.5 m. Turnaround temperatures ranged from a minimum of 603 K at the bottom to 1324.8 K. The calculated outlet fluid quality is not a strong function of the moving mesh nodalization. However, short duration spikes in the calculated quality that do occur as the coarse nodes quench can be reduced with an extended moving mesh range.

## 4. NRC/RSR DATA BANK PROGRAM

S. F. Bankert

NRC has established the NRC/Reactor Safety Research (RSR) Data Bank Program to provide the means for collecting, processing, and making available reactor safety experimental data. These data represent both foreign and domestic sources and are processed on digital tape in a standard format. Copies of these digital tapes are available from the Oak Ridge National Laboratory upon request. The data are also stored on the INEL computer system. The Data Bank Processing System (DBPS) is a collection of computer programs on the INEL computer system. These programs have been developed to provide the capability of accepting data from established data sources, outputting these data to tape in the standard format, adding these data to the

INEL computer system, and allowing on-line selective retrieval and comparison of these data to those who have access to the INEL computer system. Recent INEL user experience is leading to a shift in the direction of DBPS development to accommodate comparisons of non-Data Bank data with the NRC approved data in the Data Bank. The DBPS is continuing to be expanded to provide all Data Bank users with more powerful data processing, presentation, and analysis tools.

# VI. 3-D EXPERIMENT PROJECT

R. E. Rice, Manager

The 3-D Project has continued with the development of specialized two-phase fluid measurement instruments for safety experiments in Japan and Germany. Initial shipments of instruments have been made to Japan. Small scale air-water experiments investigating reflood hydraulics of the upper core support plate and upper plenum have been completed.

## 1. INSTRUMENTATION DEVELOPMENT

M. M. Hintze

### 1.1 JAERI Large Scale Reflood Test (LSRT) Facility

Instruments are being developed, manufactured, and tested in the 3-D Experiment Project for use in the Japanese LSRT Facility. These instruments include eight instrumented spool pieces, fifteen conductivity liquid level detector assemblies, and four downcomer drag disc assemblies. The associated signal conditioners, cables, racks, and installation equipment for each of these systems are also being finalized for delivery.

The instrumented spool piece prototype for the Japanese Atomic Energy Research Institute (JAERI) was fabricated and subjected to calibration and environmental testing in a single-phase flow facility. Preparations were made for more complex two-phase flow tests. The most significant accomplishments for the JAERI instrumented spool piece project was the development of a three-beam low-energy gamma densitometer and the design of a stand-alone microprocessor data system complete with all support systems.

Twelve of fifteen conductivity liquid level detector assemblies planned for the JAERI facility were delivered and installed. The downcomer drag disc design has progressed almost to completion. A significant technical problem solved in this task was the development

of a method of calibrating these devices in a simulated "free field" condition. A test fixture was designed such that the full-flow calibration of the test section can be related to the local "free field" condition that exists in the downcommer.

### 1.2 German Primary Coolant Loop (PKL) Test Facility

The 3-D instruments being developed, manufactured, and tested for the German PKL Facility include four instrumented spool pieces, five conductivity liquid level detector assemblies, and four upper plenum turbine flow meters along with signal conditioners and supporting equipment.

The PKL instrumented spool piece project has been conducted in parallel with the JAERI spool piece development. As in the JAERI effort, a significant accomplishment was the development of a three-beam low-energy gamma densitometer. The PKL densitometer design was similar to that of the JAERI design but, due to pipe diameter differences, required a separate and distinct development. Testing of the PKL instrumented spool prototype in single-phase flow conditions was started. The PKL system also has its own stand-alone microprocessor data system.

Preliminary design review has been completed on the upper plenum turbine flowmeter project for the PKL Facility. Simulation of a free field flow environment in calibration tests was achieved. These turbine flowmeters, like the downcomer drag discs for the JAERI LSRT Facility, will be used to measure local (or free field) velocities and will be calibrated in a full-flow test section.

## 2. AIR-WATER TESTS

C. M. Mohr

The testing and preliminary analysis phases of the 3-D Air-Water Upper Plenum Test Program were completed. The most recent tests performed, those modeling typical Westinghouse Electric Corporation upper

plenum designs, have further emphasized the influence of geometry upon the potential countercurrent flooding at the top of the core during LOCA reflood conditions. A preliminary evaluation of the test data suggest that the Westinghouse geometries employed are more restrictive to countercurrent flooding than the German KKU tested modeled previously. This tendency is displayed in Figure 22, which summarizes the results of the tests in terms of the square roots of the gas and liquid Kutateladze numbers $K_g$ and $K_\ell$. These dimensionless groups are defined in Equations (2) and (3).

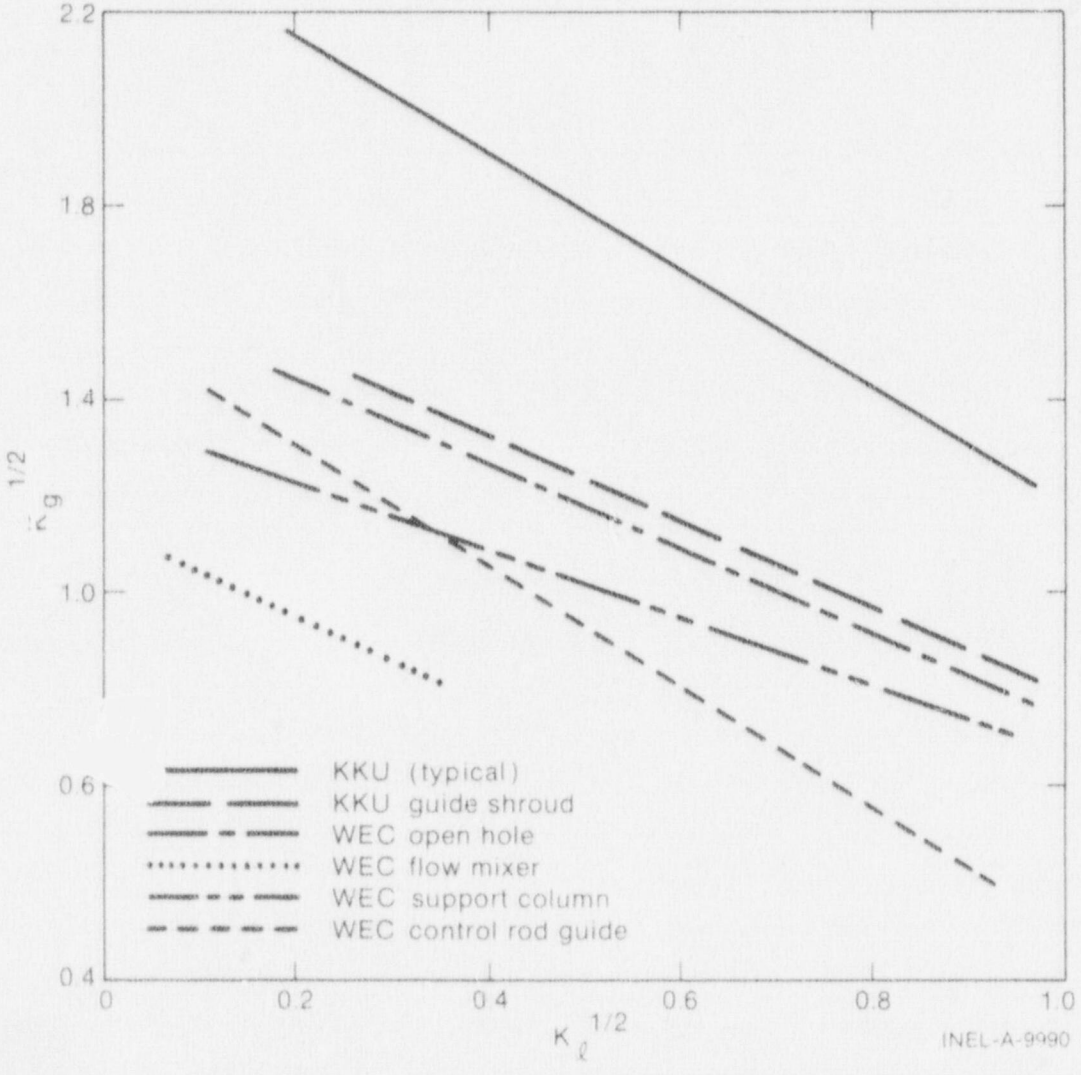


Fig. 22 Square root of Kutateladze numbers (liquid versus gas) for complete Air-Water Upper Plenum Flow Test Series for German PWR (KKU) and Westinghouse Electric Corporation (WEC) PWR flow models.

$$K_{\ell} = j_{\ell} \rho_{\ell}^{0.5} \Big/ \left[ g\sigma(\rho_{\ell} - \rho_g) \right]^{0.25} \qquad (2)$$

$$K_g = j_g \rho_g^{0.5} \Big/ \left[ g\sigma(\rho_{\ell} - \rho_g) \right]^{0.25} \qquad (3)$$

where

K = Kutateladze number

j = volumetric flux through flooding flow area (m/s)

$\rho$ = density ($kg/m^3$)

g = gravitational constant ($9.8\ m/s^2$)

$\sigma$ = surface tension (N/m)

subscripts

g = gas phase

$\ell$ = liquid phase.

The "KKU typical" line in Figure 22 represents results of the KKU open hole and support column and the JAERI upper core support plate flow models; the results were quite similar and were reported[a] as part of the results of the first four 3-D air-water upper plenum tests. From Figure 22, the curves are seen to retain the linear behavior expected when the square roots of the dimensionless groups are used.

---

[a] Reference 3, pp. 80-83.

## VII. REFERENCES


1. B. L. Collins et al, Experiment Data Report for Semiscale Mod-3 Blowdown Heat Transfer Test S-07-1 (Baseline Test Series), NUREG/CR-0281, TREE-1221 (September 1978).

2. R. L. Gillins et al, Experiment Data Report for Semiscale Mod-3 Reflood Heat Transfer Test S-07-4 (Baseline Test Series), NUREG/CR-0254, TREE-1224 (August 1978).

3. E. L. Wills (ed.), Quarterly Technical Progress Report on Water Reactor Safety Programs Sponsored by the Nuclear Regulatory Commission's Division of Reactor Safety Research, April-June 1978 NUREG/CR-0252, TREE-1219 (July 1978).

4. D. H. Freund and E. L. Wills (eds.), Quarterly Technical Progress Report on Water Reactor Safety Programs Sponsored by the Nuclear Regulatory Commission's Division of Reactor Safety Research, January-March 1978, TREE-NUREG-1218 (April 1978).

5. M. Petrick and B. S. Swanson, "Radiation Attenuation Method of Measuring Density of a Two-Phase Fluid," Rev. Sci., Instr., 29, No. 12 (1958) pp 1079-85.

6. H. S. Isbin et al, "Void Fractions in Two-Phase Flow," AICHE Journal, 5, No. 4 (1959) pp 427-432.

7. F. W. Staub et al, Heat Transfer and Hydraulics, The Effects of Subcooled Voids, NYO-3679-8 (May 1969).

8. N. Zuber et al, Steady State and Transient Void Fractions in Two-Phase Flow Systems: Final Report for the Program of Two-Phase Flow Investigation, GEAP-5417, 2 vol. (January 1967).

9. A. G. Stephens, "Determination of Flow Regime Characteristics by Photon Attenuation," Ph.D. Thesis, Pennsylvania State University, 1975.

10. G. P. Lilly, A. G. Stephens, L. E. Hochreiter, Mixing of Emergency Core Cooling Water with Steam: 1/14 Scale Testing Phase, EPRI Report 294-2 (January 1975).

11. G. D. Lassahn, LOFT Three-Beam Densitometer Data Interpretation, TREE-NUREG-1111 (October 1977).

12 K. V. Moore and W. H. Rettig, RELAP4 - A Computer Program for Transient Thermal-Hydraulic Analysis, ANCR-1127, Rev. 1 (March 1975).

13. T. Fujishiro et al, Light Water Reactor Fuel Response During Reactivity Initiated Accident Experiments, NUREG/CR-0269, TREE-1237 (August 1978).

14. D. E. Owen, Pellet-Cladding Mechanical Interactions in Halden Assembly IFA-226, NUREG/CR-0282, TREE-1266 (August 1978).

15. P. E. MacDonald, D. E. Owen, M. E. Waterman, Fuel Rod Temperature and Pressure Response in Halden Reactor Experiment IFA-226, NUREG/CR-0267, TREE-1238 (August 1978).

16. N. D. Cox, "Comparison of Two Uncertainty Analysis Methods," Nuclear Science and Engineering, 64 (September 1977) pp 258-265.

17. D. R. Coleman, "Influence of Calculated Gap Closure and Fission Product Inventory on FRAP-T4 Cladding Failure Analysis Under PCI Conditions," ENS/ANS Topical Meeting on Nuclear Power Reactor Safety, Brussels, Belgium, October 16-19, 1978.

18. Quarterly Technical Progress Report on Water Reactor Safety Programs Sponsored by the Nuclear Regulatory Commission's Division of Reactor Safety Research, October - December 1977, TREE-NUREG-1205 (April 1978).

19. D. R. Coleman and E. T. Laats, FRAP-T2: A Computer Code for the Transient Analysis of Oxide Fuel Rods, Vol. II, Model Verification Report, TREE-NUREG-1040 (March 1977).

DISTRIBUTION RECORD FOR NUREG/CR-0412
(TREE-1294

Internal Distribution

1 - Chicago Patent Group - DOE
9800 South Cass
Argonne, IL 60439

2 - R. L. Blackledge
Idaho Operations Office - DOE
Idaho Falls, ID 83401

3 - R. J. Beers, ID

4 - P. E. Litteneker, ID

5 - R. E. Tiller, ID

6 - H. P. Pearson
Information Management, EG&G

7-12 - INEL Technical Library

13-19 - Editor

20-81 - Special Internal

External Distribution

82-83 - Saul Levine, Director
Office of Nuclear Regulatory Research, NRC
Washington, D.C. 20555

84-90 - Special External

91-117 - Technical Information Center - DOE
Box 62
Oak Ridge, TN 37830

118-615 - Distribution under R2, R3, R4, Water Reactor Safety Research